Article

Chelate-Controlled Synthesis of Racemic *ansa*-Zirconocenes

Matthew D. LoCoco, Xingwang Zhang, and Richard F. Jordan

J. Am. Chem. Soc., **2004**, 126 (46), 15231-15244• DOI: 10.1021/ja046629+ • Publication Date (Web): 02 November 2004

J|A|C|S
ARTICLES
Published on Web 11/02/2004

Chelate-Controlled Synthesis of Racemic *ansa*-Zirconocenes

Matthew D. LoCoco, Xingwang Zhang, and Richard F. Jordan*

Contribution from the Department of Chemistry, The University of Chicago, 5735 South Ellis Avenue, Chicago, Illinois 60637

Received June 8, 2004; E-mail: rfjordan@uchicago.edu

Abstract: The reaction of Zr{PhN(CH$_2$)$_3$NPh}Cl$_2$(THF)$_2$ (**5**) with lithium *ansa*-bis-indenyl reagents Li$_2$[XBI](Et$_2$O) (XBI = (1-indenyl)$_2$SiMe$_2$ (SBI, **7a**), (2-methyl-1-indenyl)$_2$SiMe$_2$ (MSBI, **7b**), (2-methyl-4,5-benz-1-indenyl)$_2$SiMe$_2$ (MBSBI, **7c**), (2-methyl-4-phenyl-1-indenyl)$_2$SiMe$_2$ (MPSBI, **7d**), and 1,2-(1-indenyl)$_2$ethane (EBI, **7e**)) affords *rac*-(XBI)Zr{PhN(CH$_2$)$_3$NPh} (**8a**−**e**) in high yield. The *meso* isomers were not detected by ^{1}H NMR. X-ray crystallographic studies show that the Zr{PhN(CH$_2$)$_3$NPh} rings in **5**, **8a**, **8c**, and (C$_5$H$_5$)$_2$-Zr{PhN(CH$_2$)$_3$NPh} (**10**) adopt twist conformations that position the N−*Ph* groups on opposite sides of the N−Zr−N plane. This conformation complements the metallocene structures of *rac*-**8a**−**e** but would destabilize the corresponding *meso* isomers. It is proposed that the Zr{PhN(CH$_2$)$_3$NPh} ring adopts a similar twist conformation in the stereodetermining transition state for addition of the second indenyl ring in these reactions, which leads to a preference for *rac* products. The results of metallocene syntheses from other Zr amide precursors support this proposal. **8a**−**e** are converted to the corresponding *rac*-(XBI)ZrCl$_2$ complexes (**9a**−**e**) by reaction with HCl.

Introduction

The application of chiral group 4 *ansa*-metallocene complexes as stereoselective catalysts and reagents has been studied extensively.[1,2] However, this field is limited by the fact that many of the most interesting catalyst structures are difficult to prepare. Group 4 *ansa*-metallocenes are usually synthesized by reaction of [Cp′XCp′]$^{2-}$ reagents with MX$_4$ or MX$_4$L$_2$ compounds (eq 1; Cp′ = generic cyclopentadienyl or indenyl group; X = bridge). The factors that control chemoselectivity (i.e., metallocene vs dinuclear, oligomeric or other products) and diastereoselectivity (i.e., *rac*/*meso* selectivity) in these reactions are not well understood, and extensive screening of counterions, solvents, added ligands, and reaction conditions may be required to obtain acceptable yields. Often the procedures are tedious and the yields are low, which is particularly problematic for structurally complex bis-indenyl metallocenes, for which multistep [Cp′XCp′]$^{2-}$ ligand syntheses are required.[3] It is usually assumed that the metalation reactions are irreversible and the selectivity is kinetically controlled.

Several strategies for tailoring the [Cp′XCp′]$^{2-}$ structure to favor or dictate the formation of *rac* diastereomers or specific enantiomers have been explored, including the use of substituents in the 2,2′-Cp′ positions,[4] sterically bulky bridges,[5] stereogenic Cp′ rings or bridges,[6] and directing ligands.[7] Photochemical and thermal conversions of *rac*/*meso* mixtures to *rac*-enriched metallocenes have been reported, and in several cases were coupled with complexation to chiral auxiliaries to achieve dynamic resolutions.[7b,8] Additionally, silicon, tin, and

(1) For reviews and applications in olefin polymerization, see: (a) Brintzinger, H. H.; Fischer, D.; Mülhaupt, R.; Rieger, B.; Waymouth, R. M. *Angew. Chem., Int. Ed. Engl.* **1995**, *34*, 1143. (b) Resconi, L.; Cavallo, L.; Fait, A.; Piemontesi, F. *Chem. Rev.* **2000**, *100*, 1253. (c) Hoveyda, A. H.; Morken, J. P. *Angew. Chem., Int. Ed. Engl.* **1996**, *35*, 1262. (d) Halterman, R. L. In *Metallocenes: Synthesis, Reactivity, Applications*; Togni, A., Halterman, R. L., Eds.; Wiley-VCH: Weinheim, 1998; Vol. 1, Chapter 8, p 455. (e) Halterman, R. L. *Chem. Rev.* **1992**, *92*, 965.

(2) Olefin hydrogenation: (a) Troutman, M. V.; Appella, D. H.; Buchwald, S. L. *J. Am. Chem. Soc.* **1999**, *121*, 4916. (b) Broene, R. D.; Buchwald, S. L. *J. Am. Chem. Soc.* **1993**, *115*, 12569. (c) Waymouth, R.; Pino, P. *J. Am. Chem. Soc.* **1990**, *112*, 4911. Hydrosilylation of ketones and imines: (d) Hansen, M. C.; Buchwald, S. L. *Org. Lett.* **2000**, *2*, 713. (e) Yun, J.; Buchwald, S. L. *J. Am. Chem. Soc.* **1999**, *121*, 5640. (f) Verdaguer, X.; Lanhe, U. E. W.; Reding, M. T.; Buchwald, S. L. *J. Am. Chem. Soc.* **1996**, *118*, 6784. (g) Yun, J.; Buchwald, S. L. *Chirality* **2000**, *12*, 476. (h) Carter, M. B.; Schiøtt, B.; Gutiérrez, A.; Buchwald, S. L. *J. Am. Chem. Soc.* **1994**, *116*, 11667. Diels−Alder reactions: (i) Bondar, G. V.; Aldea, R.; Levy, C. J.; Jaquith, J. B.; Collins, S. *Organometallics* **2000**, *19*, 947. (j) Jaquith, J. B.; Guan, J.; Wang, S.; Collins, S. *Organometallics* **1995**, *14*, 1079. Olefin carbomagnesiation and carboalumination: (k) Visser, M. S.; Harrity, J. P. A.; Hoveyda, A. H. *J. Am. Chem. Soc.* **1996**, *118*, 3779. (l) Bell, L.; Whitby, R. J.; Jones, R. V. H.; Standen, M. C. H. *Tetrahedron Lett.* **1996**, *37*, 7139. (m) Bell, L.; Brookings, D. C.; Dawson, G. J.; Whitby, R. J.; Jones, R. V. H.; Standen, M. C. H. *Tetrahedron* **1998**, *54*, 14617. (n) Dawson, G.; Durrant, C. A.; Kirk, G. G.; Whitby, R. J.; Jones, R. V. H.; Standen, M. C. H. *Tetrahedron Lett.* **1997**, *38*, 2335. Pauson−Khand reactions: (o) Hicks, F. A.; Buchwald, S. L. *J. Am. Chem. Soc.* **1999**, *121*, 7026. (p) Sturla, S.; Buchwald, S. L. *J. Org. Chem.* **1999**, *64*, 5547. Olefin epoxidation: (q) Colletti, S. L.; Halterman, R. L. *J. Organomet. Chem.* **1993**, *455*, 99. Pinacol coupling: (r) Halterman, R. L.; Zhu, C.; Chen, Z.; Dunlap, M. S.; Khan, M. A.; Nicholas, K. M. *Organometallics* **2000**, *19*, 3824. Olefin−pyridine coupling: (s) Dagorne, S.; Rodewald, S.; Jordan, R. F. *Organometallics* **1997**, *16*, 5541. (t) Rodewald, S.; Jordan, R. F. *J. Am. Chem. Soc.* **1994**, *116*, 4491. Kinetic resolution of allenes: (u) Sweeney, Z. K.; Salsman, J. L.; Andersen, R. A.; Bergman, R. G. *Angew. Chem., Int. Ed.* **2000**, *39*, 2339. Synthesis of α-amino acid derivatives: (v) Gately, D. A.; Norton, J. R. *J. Am. Chem. Soc.* **1996**, *118*, 3479. Isomerization of nonfunctionalized olefins: (w) Chen, Z.; Halterman, R. *J. Am. Chem. Soc.* **1992**, *114*, 2276.

(3) For example, see: (a) Spaleck, W.; Kuber, F.; Winter, A.; Rohrmann, J.; Bachman, B.; Antberg, M.; Dolle, V.; Paulus, E. F. *Organometallics* **1994**, *13*, 954. (b) Stehling, U.; Diebold, J.; Kristen, R.; Roll, W.; Brintzinger, H. H.; Jüngling, S.; Mülhaupt, R.; Langhauser, F. *Organometallics* **1994**, *13*, 964.

(4) (a) Wiesenfeldt, H.; Reinmuth, A.; Barsties, E.; Evertz, K.; Brintzinger, H. H. *J. Organomet. Chem.* **1989**, *369*, 359. (b) Chacon, S. T.; Coughlin, E. B.; Henling, L. M.; Bercaw, J. E. *J. Organomet. Chem.* **1995**, *497*, 171. (c) Leino, R.; Luttikhedde, H.; Wilén, C.; Sillanpää, R.; Näsman, J. H. *Organometallics* **1996**, *15*, 2450. (d) Coughlin, E. B.; Bercaw, J. E. *J. Am. Chem. Soc.* **1992**, *114*, 7606.

(5) (a) Chen, Y. X.; Rausch, M. D.; Chien, J. C. W. *Organometallics* **1994**, *13*, 748.

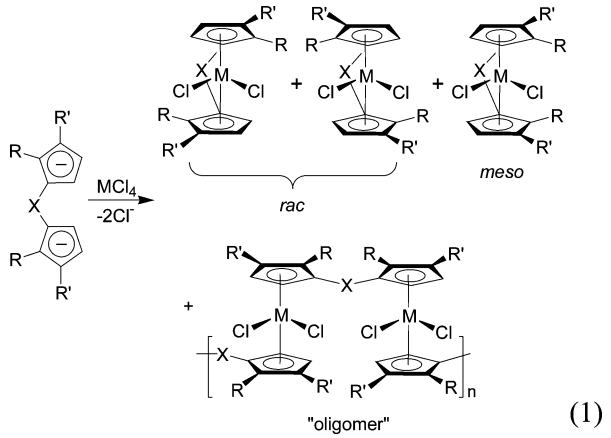

(1)

aluminum $[Cp'XCp']^{2-}$ derivatives can be used to synthesize group 4 *ansa*-metallocenes, in some cases with high *rac* selectivity.[9] However, most of these approaches are limited to specific metallocenes, and in some cases the yields are low.

Amine elimination reactions of $Zr(NMe_2)_4$ with $[Cp'XCp']H_2$ compounds provide efficient routes to simple *ansa*-zirconocenes such as *rac*-(EBI)$Zr(NMe_2)_2$ and *rac*-(SBI)$Zr(NMe_2)_2$ (EBI = 1,2-bis(1-indenyl)ethane; SBI = (1-indenyl)$_2SiMe_2$).[10] However, this approach fails for metallocenes that contain 2-Me-substituted *ansa*-bis-indenyl ligands, which are useful as high-performance propylene polymerization catalysts.[1,3]

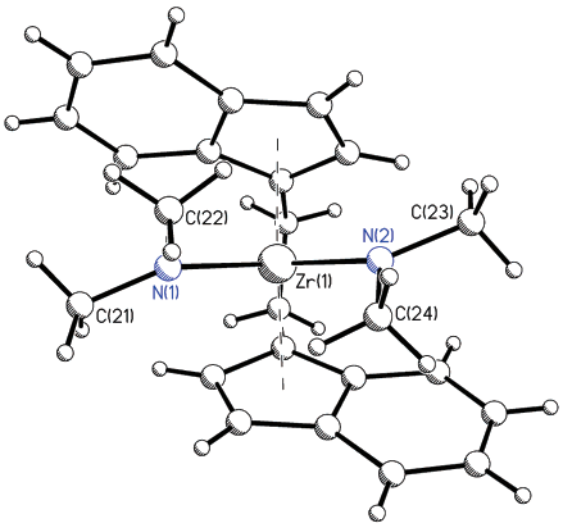

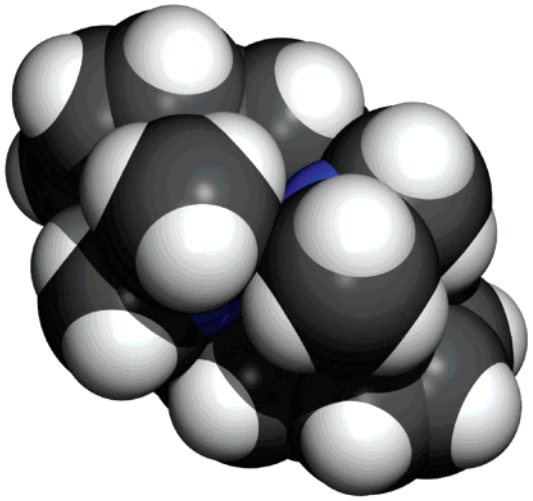

Figure 1. Molecular structure and space-filling view of *rac*-(EBI)Zr-$(NMe_2)_2$. See ref 10b.

The amide ligands of $(Cp'XCp')Zr(NR_2)_2$ complexes invariably adopt staggered arrangements in which the "outer" R substituents are directed toward the sterically open quadrants above and below the N−Zr−N plane, as illustrated for *rac*-(EBI)$Zr(NMe_2)_2$ in Figure 1.[10b] This arrangement minimizes steric crowding between the amide and indenyl ligands. The generality of this structural motif suggested that it might be possible to prepare metallocenes with high diasteroselectivity by reacting $[Cp'XCp']^{2-}$ reagents with Zr precursors that contain bulky amides constrained to the staggered orientation, i.e., by retrofitting the *ansa* ligand to a suitably designed Zr−bis-amide unit. Here we describe a general synthesis of *ansa*-bis(indenyl) zirconocenes that is based on this concept and extensive X-ray structural studies that provide insight into the stereocontrol mechanism.[11]

Results and Discussion

Ligand Preparation. The bis-amide ligand $[PhN(CH_2)_3NPh]^{2-}$ is the key to the metallocene synthesis described here. The diamine *N*,*N*′-diphenyl-1,3-propanediamine (**1**) can be prepared in several ways from 1,3-dibromopropane (**2**) as illustrated in

(6) (a) Huttenloch, M. E.; Dorer, B.; Rief, U.; Prosenc, M. H.; Schmidt, K.; Brintzinger, H. H. *J. Organomet. Chem.* **1997**, *541*, 219. (b) Grossman, R. B.; Tsai, J. C.; Davis, W. M.; Gutiérrez, A.; Buchwald, S. L. *Organometallics* **1994**, *13*, 3892. (c) Huttenloch, M. E.; Diebold, J.; Rief, U.; Brintzinger, H. H.; Gilbert, A. G.; Katz, T. J. *Organometallics* **1992**, *11*, 3600. (d) Ellis, W. W.; Hollis, T. K.; Odenkirk, W.; Whelan, J.; Ostrander, R.; Rheingold, A. L.; Bosnich, B. *Organometallics* **1993**, *12*, 4391. (e) Halterman, R. L.; Ramsey, T. M. *Organometallics* **1993**, *12*, 2879. (f) Halterman, R. L.; Chen, Z.; Khan, M. A. *Organometallics* **1996**, *15*, 3957. (g) Rheingold, A. L.; Robsinson, N. P.; Whelan, J.; Bosnich, B. *Organometallics* **1992**, *11*, 1869. (h) Rieger, B. *J. Organomet. Chem.* **1992**, *428*, C33. (i) Ramsey, T. M.; Halterman, R. L. *J. Organomet. Chem.* **1997**, *530*, 225. (j) Könemann, M.; Erker, G.; Fröhlich, R.; Kotila, S. *Organometallics* **1997**, *16*, 2900. (k) Hollis, T. K.; Rheingold, A. L.; Robinson, N. P.; Whelan, J.; Bosnich, B. *Organometallics* **1992**, *11*, 2812. (l) Colletti, S. L.; Halterman, R. L. *Organometallics* **1991**, *10*, 2998. (m) Halterman, R. L.; Combs, D.; Kihega, J. G.; Khan, M. A. *J. Organomet. Chem.* **1996**, *520*, 163. (n) Mansel, S.; Rief, U.; Prosenc, M. H.; Kirsten, R.; Brintzinger H. H. *J. Organomet. Chem.* **1996**, *512*, 225. (o) Mitchell, J. P.; Hajela, S.; Brookhart, S. K.; Hardcastle, K. I.; Henling, L. M.; Bercaw, J. E. *J. Am. Chem. Soc.* **1996**, *118*, 1045.
(7) (a) Erikson, M. S.; Fronczek, F. R.; McLaughlin, M. L. *J. Organomet. Chem.* **1991**, *415*, 75. (b) Damrau, H. R.; Royo, E.; Obert, S.; Schaper, F.; Weeber, A.; Brintzinger, H. H. *Organometallics* **2001**, *20*, 5258. (c) Chen, Y. X.; Campbell, R. E.; Devore, D. D.; Green, D.; Link, P.; Soto, B. J.; Wilson, D. R.; Abboud, K. A. *J. Am. Chem. Soc.* **2004**, *126*, 42.
(8) (a) Wild, F. R. W. P.; Zsolnai, L.; Huttner, G.; Brintzinger, H. H. *J. Organomet. Chem.* **1982**, *232*, 233. (b) Collins, S.; Hong, Y.; Taylor, N. J. *Organometallics* **1990**, *9*, 2695. (c) Schmidt, K.; Reinmuth, A.; Rief, U.; Diebold, J.; Brintzinger, H. H. *Organometallics* **1997**, *16*, 1724. (d) Hollis, T. K.; Wang, L.; Tham, F. *J. Am. Chem. Soc.* **2000**, *122*, 11737. (e) Ringwald, M.; Stürmer, R.; Brintzinger, H. H. *J. Am. Chem. Soc.* **1999**, *121*, 1524.
(9) (a) Voskoboynikov, A. Z.; Agarkov, A. Y.; Chernyshev, E. A.; Beletskaya, I. P.; Churakov, A. V.; Kuz'mina, L. G. *J. Organomet. Chem.* **1997**, *530*, 75. (b) Nifant'ev, I. E.; Ivchenko, P. V. *Organometallics* **1997**, *16*, 713. (c) Hüttenhofer, M.; Weeber, A.; Brintzinger, H. H. *J. Organomet. Chem.* **2002**, *663*, 58. (d) Hüttenhofer, M.; Schaper, F.; Brintzinger, H. H. *Angew. Chem., Int. Ed.* **1998**, *37*, 2268. (e) Thiyagarajan, B.; Jordan, R. F.; Young, V. G., Jr. *Organometallics* **1999**, *18*, 5347. (f) Thiyagarajan, B.; Jordan, R. F.; Young, V. G., Jr. *Organometallics* **1998**, *17*, 281.
(10) (a) Diamond, G. M.; Rodewald, S.; Jordan, R. F. *Organometallics* **1995**, *14*, 5. (b) Diamond, G. M.; Jordan, R. F.; Petersen, J. L. *J. Am. Chem. Soc.* **1996**, *118*, 8024. (c) Diamond, G. M.; Jordan, R. F.; Petersen, J. L. *Organometallics* **1996**, *15*, 4045. (d) Christopher, J. N.; Diamond, G. M.; Jordan, R. F.; Petersen, J. L. *Organometallics* **1996**, *15*, 4038. (e) Diamond, G. M.; Jordan, R. F.; Petersen, J. L. *Organometallics* **1996**, *15*, 4030. (f) Christopher, J. N.; Jordan, R. F.; Petersen, J. L.; Young, V. G., Jr. *Organometallics* **1997**, *13*, 33044. (g) Halterman, R. L.; Combs, D.; Khan, M. A. *Organometallics* **1998**, *17*, 3900. (h) Bravakis, A. M.; Bailey, L. E.; Pigeon, M.; Collins, S. *Macromolecules* **1998**, *31*, 1000. (i) Ashe, A. J.; Fang, X.; Kampf, J. W. *Organometallics* **1999**, *18*, 2288.
(11) Preliminary communication: Zhang, X.; Zhu, Q.; Guzei, I. A.; Jordan, R. F. *J. Am. Chem. Soc.* **2000**, *122*, 8093.

Scheme 1

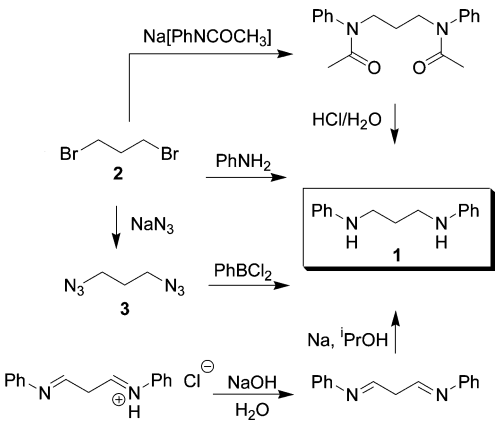

Scheme 1. The reaction of **2** with sodium acetanilide yields *N*,*N*′-diacetyl-*N*,*N*′-diphenylpropanediamine, which is converted to **1** by reaction with HCl and neutralization with NaOH.[12] However, this procedure requires the isolation of intermediates and the use of large solvent volumes. The reaction of **2** with NaN_3 yields 1,3-diazide **3**,[13] which is converted to **1** by reaction with $PhBCl_2$ followed by methanol workup and neutralization.[14] This approach is more efficient, but the use of the diazide intermediate and the expensive borane reagent limit its utility. The reaction of **2** with aniline followed by treatment with KOH yields **1** directly, and although the isolated yield is moderate, this route is useful for large-scale preparations.[15] Alternatively, reduction of malonaldehyde bis(phenylimine)·HCl with Na/2-propanol affords **1** in 95% yield on a 20 g scale.[16] Compound **1** is isolated as an oil from these reactions and may be recrystallized from toluene/hexanes. However, the oil was found to be pure by ^{1}H NMR and GC/MS and was used for all experiments described here. Deprotonation of **1** with 2 equiv of ^{n}BuLi yields $Li_2[PhN(CH_2)_3NPh]$ (**4**).

Synthesis and Structure of Zr{PhN(CH$_2$)$_3$NPh}Cl$_2$(THF)$_2$ (5). The chelated bis-amide complex $Zr\{PhN(CH_2)_3NPh\}Cl_2(THF)_2$ (**5**) is prepared as shown in Scheme 2. The reaction of $ZrCl_4$ and 2 equiv of **4** in toluene affords $Zr\{PhN(CH_2)_3NPh\}_2$ (**6**, 73%). Comproportionation of **6** and $ZrCl_4$ in THF/Et_2O yields **5** quantitatively. Alternatively, **5** can be prepared directly from $ZrCl_4$ and 1 equiv of **4** in THF/Et_2O in 86% isolated yield. The latter method was optimized for large-scale preparations.

As shown in Figure 2, **5** has approximate C_2 symmetry and octahedral geometry at Zr. The $Zr\{PhN(CH_2)_3NPh\}$ ring adopts a twist conformation (symmetric skew-boat),[17] which places the two N−*Ph* rings on opposite sides of the N−Zr−N plane. The ring conformation can be defined by the deviations of the ring atoms from the N(1)−Zr−N(2) plane (see Figure 1). The chelate ring in $Zr\{Me_3SiN(CH_2)_3NSiMe_3\}Cl_2(THF)_2$ has a similar

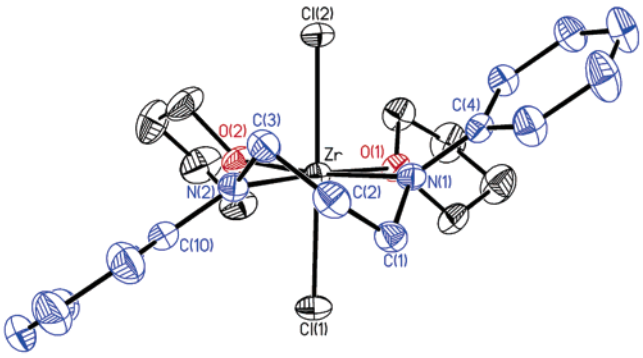

Figure 2. Molecular structure of $Zr\{PhN(CH_2)_3NPh\}Cl_2(THF)_2$ (**5**). H atoms are omitted. Bond distances (Å): Zr−N(1), 2.082(2); Zr−N(2), 2.080(2); Zr−Cl(1), 2.4785(5); Zr−Cl(2), 2.4565(5). Bond angles (deg): N(1)−Zr−N(2), 91.63(6); Cl(2)−Zr−Cl(1), 164.00(2); O(2)−Zr−O(1), 79.32(5). Sums of angles at N (deg): N(1), 358.3(3); N(2), 358.6(3). Angles between planes (deg): C(10)−N(2)−C(3)/N(2)−Zr−N(1), 36.7; C(1)−N(1)−C(4)/N(2)−Zr−N(1), 41.1. Deviations of key atoms from the N−Zr−N plane (Å): C(10), −0.722; C(3), 0.746; C(2), −0.083; C(1), −0.840; C(4), 0.771.

Scheme 2

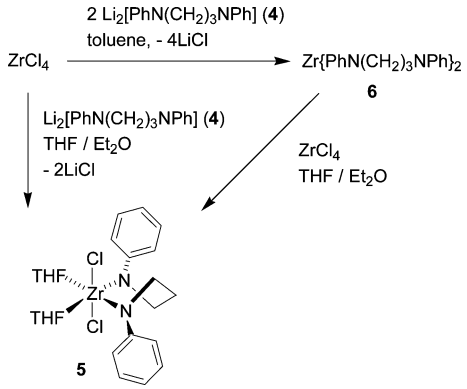

conformation.[18,19] The N−Zr−N angle in **5** is close to 90°, the geometry at each nitrogen atom is planar, and the Zr−N bond distances are normal. The ^{1}H NMR spectrum of **5** contains two methylene resonances in a 2:1 intensity ratio down to −105 °C (THF-d_8), which implies that chelate ring inversion is fast on the NMR time scale.

Synthesis of *ansa*-Zirconocenes. The reaction of **5** with $Li_2[XBI](Et_2O)$ reagents (XBI = SBI (**7a**), (2-methyl-1-indenyl)$_2$SiMe$_2$ (MSBI, **7b**), (2-methyl-4,5-benz-1-indenyl)$_2$SiMe$_2$ (MBSBI, **7c**), (2-methyl-4-phenyl-1-indenyl)$_2$SiMe$_2$ (MPSBI, **7d**), and EBI (**7e**)) in Et_2O affords the corresponding *rac*-(XBI)Zr-$\{PhN(CH_2)_3NPh\}$ zirconocenes **8a**−**e** in quantitative NMR yield and high isolated yield (Scheme 3). No significant side products were detected in these reactions. The use of Et_2O as the solvent is important. The reaction of **5** with **7c** or **7d** in THF yielded mixtures of products, possibly containing binuclear species with bridging rather than chelating $[XBI]^{2-}$ ligands, or bis-ligand species. The solubilities of **5** and **7a**−**e** in Et_2O are low, which provides high dilution conditions that favor the formation of metallocene products. Compounds **8a**−**e** are converted to the

(12) Billman, J. H.; Caswell, L. R. *J. Org. Chem.* **1951**, *16*, 1.
(13) (a) Alvarez, S. G.; Alvarez, M. T. *Synthesis* **1996**, 413. (b) Lee, J. W.; Jun, S. I.; Kim, K. *Tetrahedron. Lett.* **2001**, *42*, 2709. (c) Blumenstein, J. J.; Michejda, C. J. *Tetrahedron. Lett.* **1991**, *32*, 183.
(14) (a) Vaultier, M.; Carboni, B.; Pilar, M. *Synth. Commun.* **1992**, *22*, 665. (b) Jego, J. M.; Carboni, B.; Vaultier, M. *J. Organomet. Chem.* **1992**, *435*, 1. (c) Brown, H. C.; Midland, M. M.; Levy, A. B.; Suzuki, A.; Sono, S.; Itoh, M. *Tetrahedron* **1987**, *43*, 4079.
(15) Mimoun, H.; Saint Laumer, J. Y.; Giannini, L.; Scopelliti, R.; Floriani, C. *J. Am. Chem. Soc.* **1999**, *121*, 6158.
(16) Barluenga, J.; Cuervo, H.; Olando, B.; Fustero, S.; Gotor, V. *Synthesis* **1986**, 469.
(17) Hawkins, C. J. *Absolute Configuration of Metal Complexes*; Wiley-Interscience: New York, 1971; Chapter 1.
(18) Gade, L. H.; Freidrich, S.; Trosch, D. J. M.; Scowen, I. J.; McPartlin, M. *Inorg. Chem.* **1999**, *38*, 5295.
(19) In contrast, the chelate rings in four- and five-coordinate Zr(IV) and Ti(IV) propylenediamide complexes that contain bulky aryl or silyl *N*-substituents adopt boat conformations. (a) Scollard, J. D.; McConville, D. H.; Vittal, J. J. *Organometallics* **1995**, *14*, 5478. (b) Scollard, J. D.; McConville, D. H.; Payne, N. C.; Vittal, J. J. *Macromolecules* **1996**, *29*, 5241. (c) Lee, C. H.; La, Y.; Park, J. W. *Organometallics* **2000**, *19*, 344.

Scheme 3

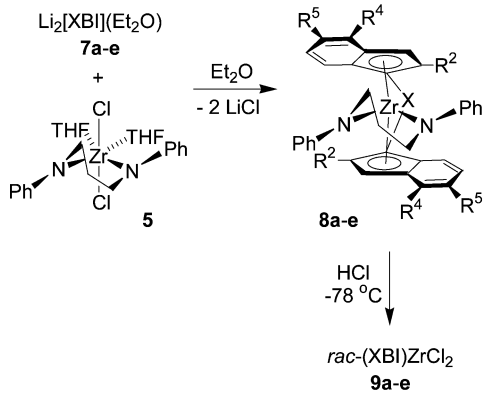

XBI ligands	8a-e Yield (%)[a]	9a-e Yield (%)[b]
a (SBI): R^2=R^4=R^5=H, X=$SiMe_2$	92	89
b (MSBI): R^2=Me; R^4=R^5=H, X=$SiMe_2$	96	76[c]
c (MBSBI): R^2=Me; R^4& R^5=benzo, X=$SiMe_2$	92	83
d (MPSBI): R^2=Me; R^4=Ph, R^5=H, X=$SiMe_2$	99	83
e (EBI): R^2=R^4=R^5=H, X=CH_2CH_2	78	81

[a] Isolated yield based on **5**. [b] Isolated yield based on **8**. [c] Isolated yield based on $ZrCl_4$ for a one-pot sequence starting from $ZrCl_4$.

corresponding dichlorides **9a**−**e** in high yield by reaction with HCl in Et_2O.

Molecular Structures of *rac*-8a and *rac*-8c. The molecular structures of two representative *rac*-(XBI)Zr{PhN$(CH_2)_3$NPh} complexes, **8a** (Figure 3) and **8c** (Figure 4), were determined to probe the stereocontrol mechanism in Scheme 3. Compounds **8a**,**c** have approximate C_2 symmetry. Significantly, in both cases, the Zr{PhN$(CH_2)_3$NPh} rings adopt twist conformations that are very similar to that of **5**. Space-filling views (Figures 3 and 4) show how this conformation complements the chiral metallocene structures. These views also suggest that significant perturbation of the Zr{PhN$(CH_2)_3$NPh} ring conformation and/or the Zr−indenyl bonding would be required to accommodate the *meso*-metallocene.

The Zr−centroid distances and the centroid−Zr−centroid angle in *rac*-**8a** (Figure 3) differ only slightly from the corresponding values for *rac*-(SBI)$ZrCl_2$ (2.224 Å, 127.81°).[20] Similarly, the Zr−centroid distances and the centroid−Zr−centroid angle in *rac*-**8c** (Figure 4) are similar to the corresponding values for *rac*-(MBSBI)$ZrCl_2$ (2.247 Å, 127.9°).[3b] The similarity of these structural data reflects the close steric matching between the metallocene and the bis-amide units in *rac*-**8a** and *rac*-**8c**.[21]

Stereocontrol Mechanism. The detailed mechanism by which the $[XBI]^{2-}$ ligand displaces the chloride and THF groups of **5** in Scheme 3 is unknown and may be complex due to ion-pairing and solvation effects and the possible role of η^1- and η^3-indenyl intermediates.[4a] However, the simple model in Scheme 4 provides useful insights. It is likely that the metallocene is formed in a stepwise process by successive, irreversible

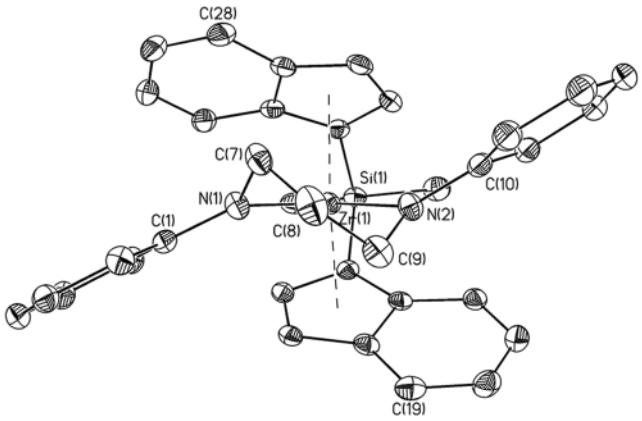

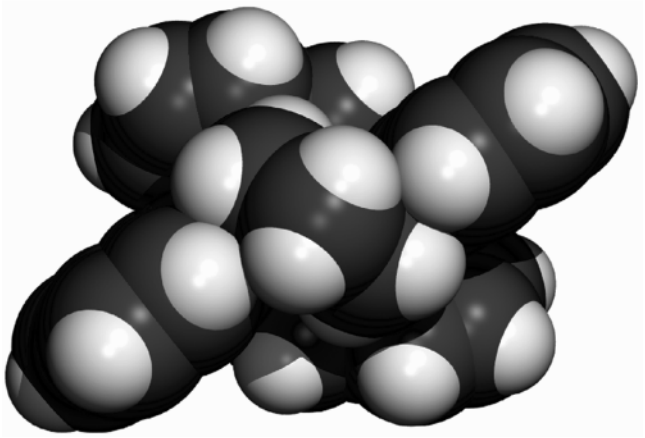

Figure 3. Molecular structure and corresponding space-filling view of *rac*-(SBI)Zr{PhN$(CH_2)_3$NPh} (*rac*-**8a**). H atoms are omitted from the ORTEP view. Bond distances (Å): Zr−N(1), 2.113(2); Zr−N(2), 2.130(2); Zr−centroid(1), 2.284; Zr−centroid(2), 2.262. Bond angles (deg): N(1)−Zr−N(2), 90.60(9); centroid(1)−Zr−centroid(2), 124.9. Sums of angles at N (deg): N(1), 359.7(4); N(2), 358.5(4). Angles between planes (deg): C(10)−N(2)−C(9)/N(1)−Zr−N(2), 36.0; C(1)−N(1)−C(7)/N(1)−Zr−N(2), 36.8. Deviations of key atoms from the N−Zr−N plane (Å): C(1), −0.621; C(7), 0.817; C(8), −0.080; C(9), −0.706; C(10), 0.721.

additions of the two indenyl ligands. The diastereoselectivity is set at the second indenyl addition and is probably kinetically controlled. As noted above, the Zr{PhN$(CH_2)_3$NPh} ring of **5** inverts rapidly. However, the flexibility of the chelate ring is probably diminished in mono-indenyl intermediate **A** and in the stereodetermining transition state linking **A** to the metallocene product, due to increased steric crowding. We postulate that the bridge (X) must be close to the "back" position in this transition state, as required in the rigid *ansa*-metallocene product, and that steric interactions between the coordinated indenyl group and the N−Ph groups favor a complementary twist conformation of the chelate ring.[22] As the second indenyl adds, steric interactions between the incoming indenyl group and the N−Ph groups block path (ii), which leads to the *meso* product, and the *rac* product forms by path (i). Unfavorable distortions of the bis-indenyl Zr unit and/or distortion of the Zr{PhN$(CH_2)_3$NPh} ring from the favored twist conformation would be required to form the *meso* isomer.

Synthesis and Structure of Cp_2Zr{PhN$(CH_2)_3$NPh}. A key hypothesis that underlies the proposed stereocontrol mechanism in Scheme 4 is that the most stable conformation of a

(20) Herrmann, W. A.; Rohrmann, J.; Herdtweck, E.; Spaleck, W.; Winter, A. *Angew. Chem., Int. Ed. Engl.* **1989**, *28*, 1511.

(21) Closest contacts between the SBI and bis-amide ligands in *rac*-**8a** (Å): H(7B)−H(28), 2.46; H(9B)−H(19), 2.44; H(15)−H(25), 2.27; H(16)−H(2), 2.29; H(7B)−C(28), 2.62; H(9B)−C(19), 2.54. Closest contacts between the MBSBI and bis-amide ligands in *rac*-**8c** (Å): H(7B)−C(43), 2.62; H(9B)−C(28), 2.64; H(15)−C(23), 2.78; H(5)−C(37), 2.75.

(22) The Zr{$Me_3SiN(CH_2)_3NSiMe_3$} chelate ring in the mono-Cp complex Zr{$Me_3SiN(CH_2)_3NSiMe_3$}(Cp){$RuCp(CO)_2$} has a twist conformation. See ref 18.

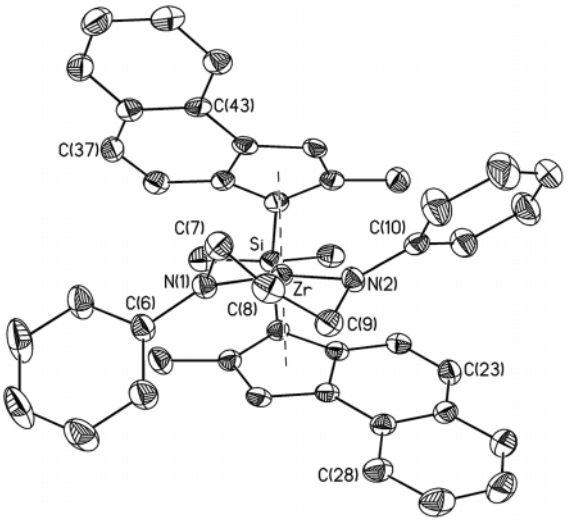

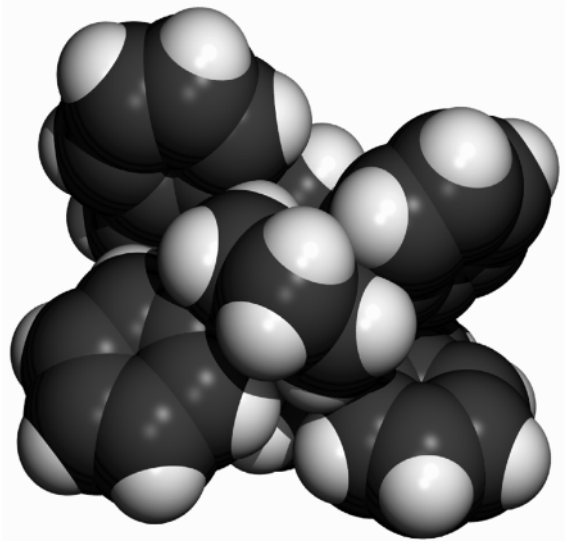

Figure 4. Molecular structure and corresponding space-filling view of *rac*-(MBSBI)Zr{PhN(CH$_2$)$_3$NPh} (*rac*-**8c**). H atoms are omitted from the ORTEP view. Bond distances (Å): Zr−N(1), 2.073(2); Zr−N(2), 2.122(2); Zr−centroid(1), 2.342; Zr−centroid(2), 2.291. Bond angles (deg): N(1)−Zr−N(2), 86.77(9); centroid(1)−Zr−centroid(2), 123.1. Sums of angles at N (deg): N(1), 359.3(4); N(2), 359.5(4). Angles between planes (deg): C(10)−N(2)−C(9)/N(1)−Zr−N(2), 32.6; C(6)−N(1)−C(7)/N(1)−Zr−N(2), 37.8. Deviations of atoms from the N−Zr−N plane (Å): C(6), −0.719; C(7), 0.852; C(8), 0.116; C(9), −0.667; C(10), 0.639.

Zr{PhN(CH$_2$)$_3$NPh)} ring in the absence of strong steric interactions is the twist conformation. To confirm this point, the parent zirconocene Cp$_2$Zr{PhN(CH$_2$)$_3$NPh} (**10**) was examined. Complex **10** was prepared by the reaction of **4** and Cp$_2$ZrCl$_2$. As shown in Figure 5, the chelate ring in **10** does adopt a twist conformation.[23] The pattern of deviations of key atoms from the N−Zr−N plane, the N−Zr−N angle, and the Zr−N distances of **10** are very similar to those for **5**, **8a**, and **8c**. The geometry of the Cp$_2$Zr unit in **10** is only minimally perturbed from that of Cp$_2$ZrCl$_2$.[24]

Synthesis and Structure of Zr(NMePh)$_2$Cl$_2$(THF)$_2$ (11). A second hypothesis of the mechanism in Scheme 4 is that the positioning of the N−*Ph* rings on opposite sides of the N−Zr−N plane in the stereodetermining transition state for addition of the second indenyl ring, which is enforced by the chelate structure, leads to a preference for the *rac* product. To probe this issue, we first examined the reactivity of Zr(NMePh)$_2$Cl$_2$(THF)$_2$ (**11**), a nonchelated analogue of **5**. Complex **11** was prepared by reaction of Zr(NMePh)$_4$ and ZrCl$_4$. As shown in Figure 6, **11** has a distorted octahedral structure with crystallographically imposed C_2 symmetry. The amide ligands adopt a staggered arrangement, with the two N−*Ph* groups at the "outside" positions (i.e., each N−Ph bond is anti to the other Zr−N bond) on opposite sides of the N−Zr−N plane. While the N−Zr−N angle in **11** is 12.9° larger than that in **5**, the Zr−N bond distances, the rotational conformation of the amide ligands, and the patterns of displacements of the N−*Ph* and N−*Me* (or N−*CH$_2$*) groups from the N−Zr−N plane are similar in the two complexes.

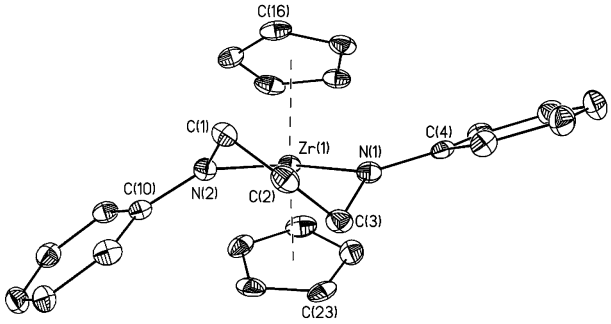

Figure 5. Molecular structure of Cp$_2$Zr{PhN(CH$_2$)$_3$NPh} (**10**). H atoms are omitted. Bond distances (Å): Zr−N(1), 2.122(3); Zr−N(2), 2.137(2); Zr−centroid(1), 2.251; Zr−centroid(2), 2.264. Bond angles (deg): N(1)−Zr−N(2), 89.57(9); centroid(1)−Zr−centroid(2), 126.0. Sums of angles at N (deg): N(1), 359.8(4); N(2), 358.7(4). Angles between planes (deg): C(4)−N(1)−C(3)/N(1)−Zr−N(2), 32.1; C(10)−N(2)−C(1)/N(1)−Zr−N(2), 42.2. Deviations of atoms from the N(2)−Zr(1)−N(1) plane (Å): C(10), −0.754; C(1), 0.714; C(2), 0.021; C(3), −0.776; C(4), 0.447.

Scheme 4 [a]

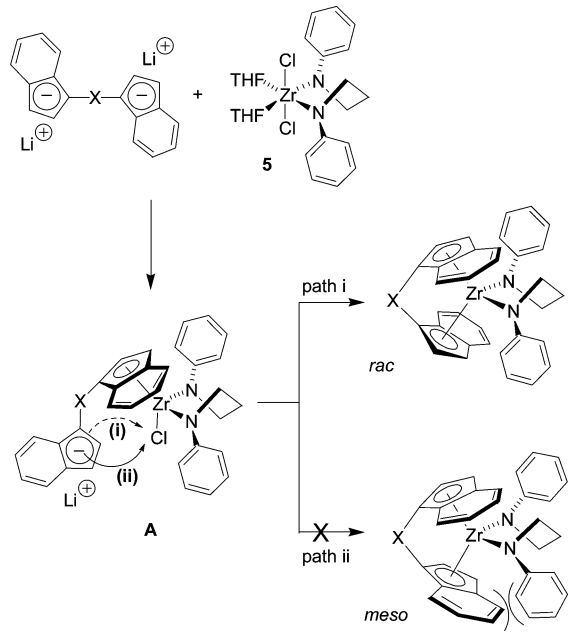

[a] X = SiMe$_2$, CH$_2$CH$_2$.

Synthesis of *ansa*-Zirconocenes Using Zr(NMePh)$_2$Cl$_2$(THF)$_2$ (11). The reaction of **11** with **7c** in Et$_2$O yields a mixture of *rac*- and *meso*-(MBSBI)Zr(NMePh)$_2$ (*rac*- and *meso*-**12**) and

(23) Closest contacts between the Cp and bis-amide ligands in **10** (Å): H(1B)−H(16), 2.27; H(3B)−H(23), 2.34; H(15)−H(25), 2.50; H(5)−H(17), 2.57.
(24) Data for Cp$_2$ZrCl$_2$: Zr−centroid distance = 2.20 Å; centroid−Zr−centroid angle = 126.0°. Prout, K.; Cameron, T. S.; Forder, R. A.; Critchley, S. R.; Denton, B.; Rees, G. V. *Acta Crystallogr. B* **1974**, *30*, 2290.

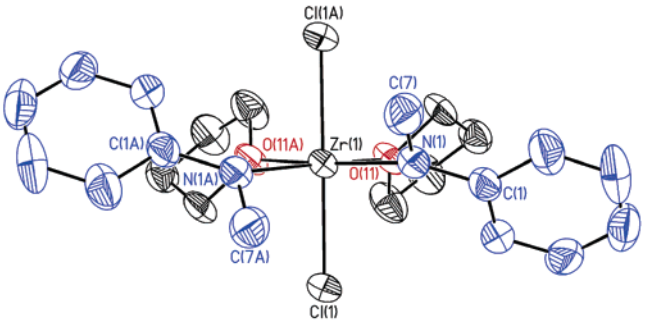

Figure 6. Molecular structure of $Zr(NMePh)_2Cl_2(THF)_2$ (**11**). H atoms are omitted. Bond distances (Å): Zr−N(1), 2.094(2); Zr−Cl(1), 2.4827(7). Bond angles (deg): N(1)−Zr−N(1A), 104.5(1); O(11)−Zr−O(11A), 77.4(1); Cl(1)−Zr−Cl(1A), 165.62(4). Sum of angles at N(1), 358.8(3)°. Angle between planes: C(1)−N(1)−C(7)/N(1)−Zr−N(1A), 39.8°. Displacements of atoms from the N(1A)−Zr(1)−N(1) plane (Å): C(1), −0.494; C(7), 0.928.

Scheme 5

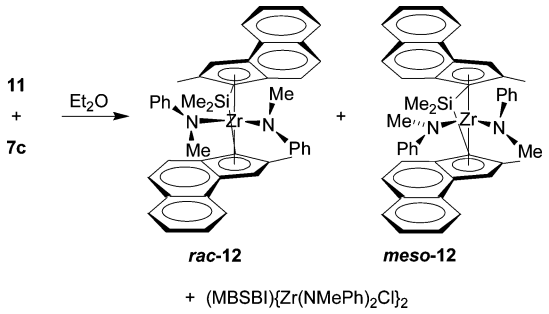

a third species assigned as the dinuclear complex (MBSBI)-$\{Zr(NMePh)_2Cl\}_2$ in a 2:2:1.5 molar ratio (Scheme 5). *rac*- and *meso*-**12** were isolated and fully characterized, and a species with the same ^{1}H NMR spectrum as the third species was generated independently by the reaction of **7c** with 2 equiv of **11**.

The structure of *rac*-**12** (Figure 7) is very similar to that of the chelated analogue **8c**. *rac*-**12** has approximate C_2 symmetry, and the amide ligands adopt a staggered arrangement that places the N−*Ph* groups in the outside positions above and below the N−Zr−N plane, in the open quadrants defined by the *rac*-metallocene unit. The N1−Zr−N2 angle is ca. 12° smaller than that in **11**, and as a result the amide ligands are rotated ca. 6.8° farther from the N−Zr−N plane.[25]

The structure of *meso*-**12** is shown in Figure 8. Due to the severe steric crowding on one side of the *meso*-metallocene unit, the arrangement of the NMePh ligands is quite different from those in **11** and *rac*-**12**. The N(1) amide ligand of *meso*-**12** is rotated only ca. 31.5° out of the N(1)−Zr−N(2) plane (vs 39−48° for **11** and *rac*-**12**), and the C(32) phenyl group occupies the "inside" position (i.e., the N(1)−C(32) bond is syn to the Zr−N(2) bond). The N(2) amide ligand is rotated 70.4° out of the N(1)−Zr−N(2) plane. This arrangement minimizes steric crowding between the C(32) phenyl group and the *meso*-(MBSBI)Zr unit and between the two amide ligands, and also results in a *face*−*face* π-stacking interaction between the C(32) phenyl ring and the C(24)−C(29) ring.[26] *meso*-**12** also differs from *rac*-**12** in that it displays significant slippage of one indenyl ring toward η^3 coordination. The indenyl slippage can be

(25) Closest contacts between the MBSBI and amide ligands in *rac*-**12** (Å): H(3)−C(37), 2.51; H(19)−C(40), 2.59.

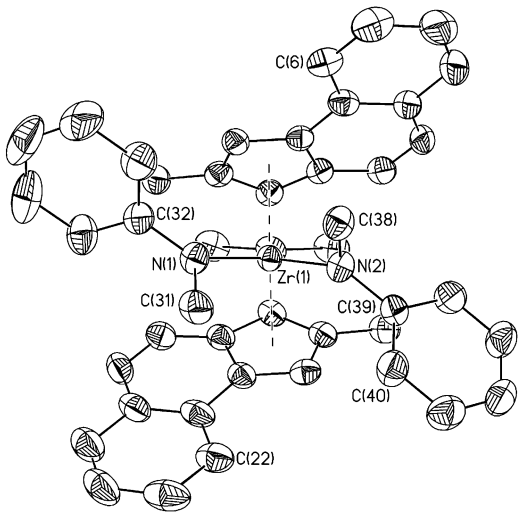

Figure 7. Molecular structure of *rac*-(MBSBI)Zr(NMePh)$_2$ (*rac*-**12**). H atoms are omitted. Bond distances (Å): Zr−N(1), 2.112(4); Zr−N(2), 2.091(4); Zr−centroid(1), 2.32; Zr−centroid(2), 2.32. Bond angles (deg): N(1)−Zr−N(2), 92.5(2); centroid−Zr−centroid, 122.26. Sums of angles at N (deg): N(1), 359.8(4); N(2), 359.8(4). Angles between planes (deg): C(32)−N(1)−C(31)/N(1)−Zr−N(2), 45.4; C(38)−N(2)−C(39)/N(1)−Zr−N(2), 47.8. Deviations of atoms from the N(1)−Zr−N(2) plane (Å): C(32), 0.768; C(31), −0.899; C(38), 0.930; C(39), −0.817.

quantified by the slip parameter Δ_{ave}(M−C), which is the difference between the average of the M−C8 and M−C9 bond lengths and the average of the M−C1, M−C2, and M−C3 bond lengths, using the labeling scheme in structure **B**.[27] The Δ_{ave}(M−C) value for the C(1)−C(13) benzindenyl ligand of *meso*-**12** is 0.14 Å, whereas the values for the C(17)−C(29) benzindenyl of *meso*-**12** and the benzindenyl ligands of *rac*-**12** and *rac*-**8c** are in the range 0.024−0.072 Å.

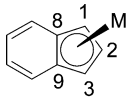

B

These results show that *meso*-**12** can form because rotations around the Zr−NMePh bonds relieve N−Ph/indenyl steric interactions on the crowded side of the metallocene while minimizing steric interactions between the two amide ligands. In contrast, in Scheme 4, the three-carbon bridge that links the amide ligands prevents rotations of this type.

Synthesis and Structure of $\{Zr\{PhN(CH_2)_2NPh\}Cl_2(THF)\}_2$ (13). Another approach to assessing the importance of the "up/down" arrangement of the N−*Ph* phenyl groups for stereocontrol in Scheme 4 is to investigate bis-amide ligands that restrict these groups to other orientations. Accordingly, we examined the use of a $Zr\{PhN(CH_2)_2NPh\}$ ring as a directing unit in *ansa*-zirconocene synthesis. The complex $\{Zr\{PhN(CH_2)_2NPh\}Cl_2(THF)\}_2$ (**13**) was prepared by reaction of $Zr\{PhN(CH_2)_2NPh\}_2$ and $ZrCl_4$. In the solid state, **13** has a dimeric structure in which two distorted octahedral Zr{PhN-

(26) (a) The distances between the carbons of the C(32) phenyl ring and the plane of the C(24)−C(29) ring range from 2.82 Å (C(36), C(37)) to 3.45 Å; ave = 3.13 Å. (b) Closest contacts between the MBSBI and amide ligands in *meso*-**12** (Å): H(38B)−H(19), 2.23; H(38B)−H(30C), 2.37; H(31B)−C(7), 2.60; H(31B)−C(6), 2.65; H(31B)−C(3), 2.71.

(27) (a) Faller, J. W.; Crabtree, R. H.; Habib, A. *Organometallics* **1985**, *4*, 929. (b) Casey, C. P.; O'Connor, J. M. *Organometallics* **1985**, *4*, 384. (c) Casey, C. P.; O'Connor, J. M. *Chem. Rev.* **1987**, *87*, 307.

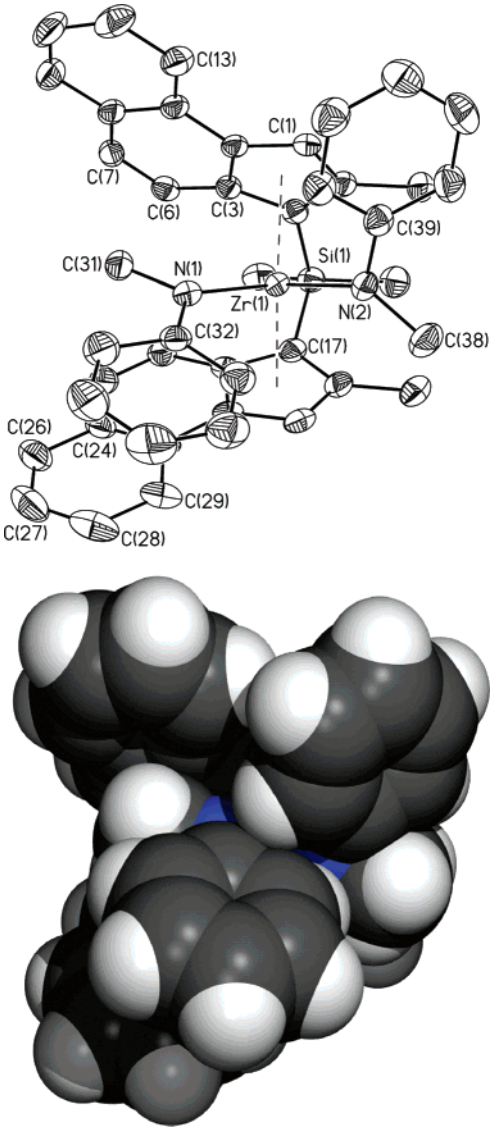

Figure 8. Molecular structure and corresponding space-filling view of *meso*-(MBSBI)Zr(NMePh)$_2$ (*meso*-**12**). H atoms are omitted from the ORTEP view. Bond distances (Å): Zr(1)−N(1), 2.137(3); Zr(1)−N(2), 2.111(3); Zr(1)−centroid(1), 2.380; Zr(1)−centroid(2), 2.310. Bond angles (deg): N(1)−Zr(1)−N(2), 98.33(1); centroid(1)−Zr(1)−centroid(2), 122.8. Sums of angles (deg): N(1), 358.1(4); N(2), 359.7(4). Angles between planes (deg): C(31)−N(1)−C(32)/N(1)−Zr(1)−N(2), 31.5; C(39)−N(2)−C(38)/N(1)−Zr(1)−N(2), 70.4. Deviations of atoms from N(1)−Zr−N(2) plane (Å): C(31), 0.533; C(32), −0.687; C(39), 1.207; C(38), −0.996.

$(CH_2)_2NPh\}Cl_2(THF)$ units are linked by chloride bridges (Figure 9). The Zr{PhN$(CH_2)_2$NPh} rings in **13** adopt envelope conformations, which place the N−*Ph* rings on the *same* side of the N−Zr−N planes and are flatter than the twist conformations of the Zr{PhN$(CH_2)_3$NPh} rings in **5**, *rac*-**8a**, *rac*-**8c**, and **10**.[28] The N−Zr−N angles in **13** are ca. 81°, which results in a sterically open environment at Zr that may favor crystallization of **13** as a dimer. Complex **13** probably exists as solvated monomers in solution, but this issue was not addressed.

Synthesis of *ansa*-Zirconocenes Using {Zr{PhN$(CH_2)_2$NPh}-Cl_2(THF)}$_2$ (13). The reaction of **13** with **7c** yields a 2:1 mixture

(28) In each Zr{PhN$(CH_2)_2$NPh} ring of **13**, the two C atoms, the Zr atom, and one N atom form a plane while the second N atom is displaced from this plane. Deviations from the C(2)−C(1)−N(1)−Zr(1) plane (Å): C(2), 0.002; C(1), 0.004; N(1), 0.003; Zr(1), 0.002; N(2), −0.564. Deviations from the C(15)−C(16)−N(4)−Zr(2) plane (Å): C(15), 0.011; C(16), 0.020; N(4), 0.017; Zr(2), 0.008; N(3), −0.566.

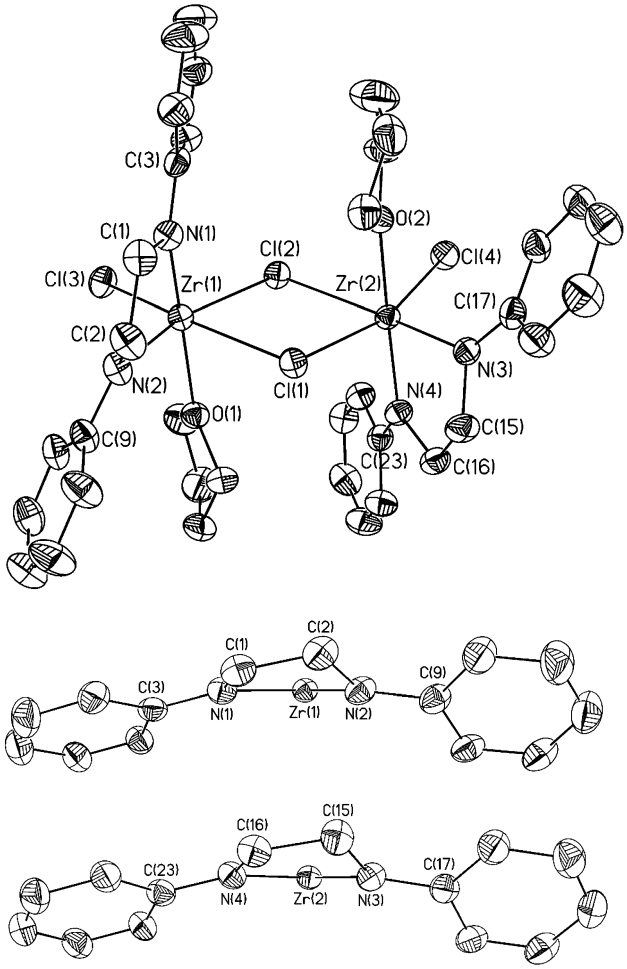

Figure 9. Molecular structure and views of the chelate rings of {Zr{PhN-$(CH_2)_2$NPh}Cl_2(THF)}$_2$ (**13**). H atoms are omitted. Bond distances (Å): Zr(1)−N(1), 2.073(2); Zr(1)−N(2), 2.046(2); Zr(2)−N(3), 2.050(2); Zr(2)−N(4), 2.071(2). Bond angles (deg): N(1)−Zr(1)−N(2), 80.86(8); N(3)−Zr(2)−N(4), 80.88(8). Sums of angles at N (deg): N(1), 359.5(3); N(2), 356.8(3); N(3), 357.5(3); N(4), 360.1(3). Angles between planes (deg): C(3)−N(1)−C(1)/N(1)−Zr(1)−N(2), 17.4; C(2)−N(2)−C(9)/N(1)−Zr(1)−N(2), 28.3; C(23)−N(4)−C(16)/N(4)−Zr(2)−N(3), 18.7; C(15)−N(3)−C(17)/N(4)−Zr(2)−N(3), 28.8. Deviations of atoms from the N(1)−Zr(1)−N(2) plane (Å): C(3), −0.360; C(1), 0.370; C(2), 0.681; C(9), −0.158. Deviations of atoms from the N(3)−Zr(2)−N(4) plane (Å): C(23), −0.353; C(16), 0.424; C(15), 0.691; C(17), −0.206.

Scheme 6

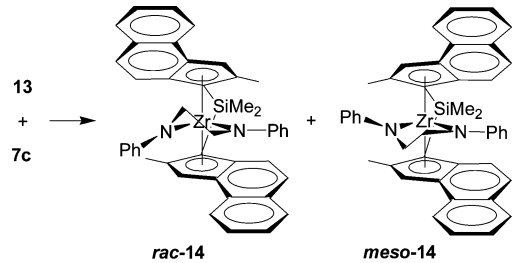

of *rac*- and *meso*-(MBSBI)Zr{PhN$(CH_2)_2$NPh} (*rac*- and *meso*-**14**, Scheme 6). Thus, the Zr{PhN$(CH_2)_2$NPh} chelate does not direct the formation of *rac* product efficiently.

The structure of *rac*-**14** is shown in Figure 10. The Zr{PhN-$(CH_2)_2$NPh} ring conformation is similar to but somewhat more puckered than those in **13**. The N(1) amide unit lies almost in the N−Zr−N plane, which allows for a π-stacking interaction between the C(3) phenyl ring and the C(35)−C(40) ring of the

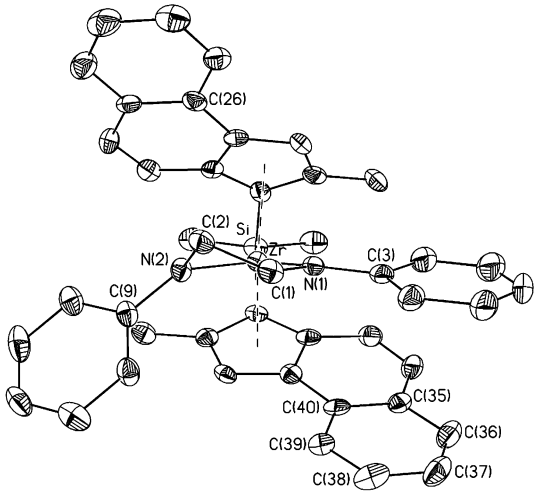

Figure 10. Molecular structure of *rac*-(MBSBI)Zr{PhN$(CH_2)_2$NPh} (*rac*-**14**). H atoms are omitted. Bond distances (Å): Zr−N(1), 2.149(3); Zr−N(2), 2.072(3); Zr−centroid(1), 2.337; Zr−centroid(2), 2.274. Bond angles (deg): N(1)−Zr−N(2), 81.3(1); centroid(1)−Zr−centroid(2), 122.8. Sums of angles at N (deg): N(1), 359.3(4); N(2), 354.4(4). Angles between planes (deg): C(9)−N(2)−C(2)/N(2)−Zr−N(1), 38.7; C(1)−N(1)−C(3)/N(2)−Zr−N(1), 8.5. Deviations of atoms from the N(1)−Zr−N(2) plane (Å): C(9), −0.831; C(2), 0.629; C(1), 0.024; C(3), −0.198.

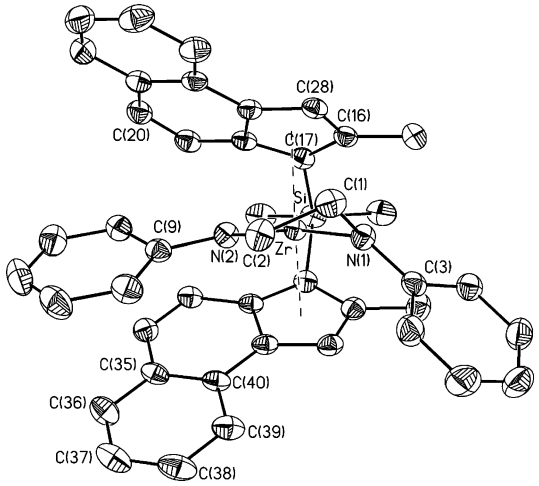

Figure 11. Molecular structure of *meso*-(MBSBI)Zr{PhN$(CH_2)_2$NPh} (*meso*-**14**). H atoms are omitted. Bond distances (Å): Zr−N(1), 2.096(2); Zr−N(2), 2.141(2); Zr−centroid(1), 2.352; Zr−centroid(2), 2.272. Bond angles (deg): N(2)−Zr−N(1), 81.40(6); centroid(1)−Zr−centroid(2), 122.6. Sums of angles at N (deg): N(1), 353.4(4); N(2), 358.8(4). Angles between planes (deg): C(9)−N(2)−C(2)/N(2)−Zr−N(1), 13.1; C(1)−N(1)−C(3)/N(2)−Zr−N(1), 42.5. Deviations of atoms from the N(2)−Zr−N(1) plane (Å): C(9), −0.318; C(2), 0.122; C(1), 0.737; C(3), −0.876.

MBSBI ligand.[29] The N(2) amide unit is rotated 38.7° out of the N−Zr−N plane, which positions the C(9) phenyl ring in an open quadrant of the *ansa*-metallocene unit. The Zr−N(2) bond is ca. 0.08 Å shorter than the Zr−N(1) bond, which may reflect differences in N−Zr π-bonding.[30] However, the chelate ring in *rac*-**14** is flexible since this species exhibits C_2 symmetry on the ^{1}H NMR time scale at room temperature.

The structure of *meso*-**14** is shown in Figure 11. The Zr{PhN$(CH_2)_2$NPh} ring is slightly more puckered than that in *rac*-**14**. The in-plane C(9) phenyl group is sandwiched between the indenyl groups on the crowded side of the *meso*-metallocene, which allows for a π-stacking interaction with the C(35)−C(40) ring.[31] The C(16)−C(28) benzindenyl ligand displays significant slippage toward η^3 coordination (Δ_{ave}(M−C) = 0.162 Å vs −0.010 to −0.031 Å for the other benzindenyl ligands in *meso*-**14** and *rac*-**14**).

These results suggest that the poor directing ability of the Zr{PhN$(CH_2)_2$NPh} ring for the *rac*-metallocene product results from the envelope conformation, which places one N−*Ph* ring in the N−Zr−N plane in an orientation that can accommodate the *meso*-metallocene.

Conclusions

The reaction of Zr{PhN$(CH_2)_3$NPh}$Cl_2(THF)_2$ (**5**) with Li_2[XBI](Et_2O) reagents **7a**−**e** provides efficient access to *rac*-(XBI)Zr{PhN$(CH_2)_3$NPh} complexes. This synthesis works well for $SiMe_2$- and CH_2CH_2-bridged XBI^{2-} ligands, and the metallocene products can be converted to the corresponding *rac*-(XBI)$ZrCl_2$ complexes in high yield by protolytic removal of the bis-amide directing ligand.

Structural studies of zirconium complexes containing chelated and nonchelated amide ligands provide insight into the factors that control diastereoselectivity in *rac*-*ansa*-zirconocene syntheses based on **5**. The most stable conformation of a Zr{PhN$(CH_2)_3$NPh} ring is the twist conformation, which positions the N−*Ph* groups on opposite sides of the N−Zr−N plane. The Zr{PhN$(CH_2)_3$NPh} twist conformation is matched to the *rac*-metallocene frameworks of *rac*-**8a**−**e** but is incompatible with the *meso* isomers due to steric crowding between the N−*Ph* and indenyl groups. It is proposed that the Zr{PhN$(CH_2)_3$NPh} ring adopts a twist conformation in the stereodetermining transition state for addition of the second indenyl ring in the reactions of **5** with **7a**−**e**, which leads to a preference for *rac* product.

In contrast, the reaction of $Zr(NMePh)_2Cl_2(THF)_2$ (**11**) with **7c** yields a mixture of *rac*- and *meso*-(MBSBI)$Zr(NMePh)_2$ (*rac*- and *meso*-**12**), along with a third species assigned as (MBSBI)-{$Zr(NMePh)_2Cl$}$_2$. *meso*-**12** can form in this reaction because Zr−NMePh bond rotations and an η^3-slip distortion of one indenyl ligand relieve N−Ph/indenyl steric interactions on the crowded side of the *meso*-zirconocene. The structure of *meso*-**12** suggests that significant perturbation of the Zr{PhN$(CH_2)_3$NPh} ring from the favored twist conformation, and possibly η^3-slippage of an indenyl ligand, would be required to form *meso*-**8a**−**e**. The reaction of {Zr{PhN$(CH_2)_2$NPh}$Cl_2(THF)$}$_2$ (**13**) with **7c** yields a mixture of *rac*- and *meso*-(MBSBI)Zr-{PhN$(CH_2)_2$NPh} (*rac*- and *meso*-**14**). The Zr{PhN$(CH_2)_2$NPh} rings in **13** and *rac*- and *meso*-**14** adopt envelope conformations that place one N−Ph ring in the N−Zr−N plane in an orientation that can accommodate the *meso*-zirconocene. These results support the proposed key role of the Zr{PhN$(CH_2)_3$NPh} twist conformation in *rac*-zirconocene syntheses using **5**.

(29) (a) The distances between the carbons of the C(3) phenyl ring and the plane of the C(35)−C(40) ring range from 3.21 Å (C(3)) to 3.72 Å (C(5)); ave = 3.47 Å. Closest contacts between the MBSBI and bis-amide ligands in *rac*-**14** (Å): H(8)−H(15C), 2.38; H(8)−H(15A), 2.39; H(2B)−C(26), 2.56.

(30) As the Zr LUMO is localized in the N−Zr−N plane, increased N−Zr π-donation is expected as the angle between the R−N−R and N−Zr−N planes increases. (a) Lauher, J. W.; Hoffmann, R. *J. Am. Chem. Soc.* **1976**, *98*, 1729. (b) Petersen, J. L.; Lichtenberger, D. L.; Fenske, R. F.; Dahl, L. F. *J. Am. Chem. Soc.* **1975**, *97*, 6433. (c) Green, J. C.; Green, M. L. H.; Prout, C. K. *J. Chem. Soc., Chem. Commun.* **1972**, 421.

(31) (a) The distances between the carbons of the C(9) phenyl ring and the plane of the C(35)−C(40) ring range from 3.05 Å (C(14)) to 3.47 Å (C(11)); ave = 3.27 Å. Closest contacts between the MBSBI and bis-amide ligands in *meso*-**14** (Å): H(1A)−H(28), 2.19; H(4)−H(29B), 2.42; H(14)−C(20), 2.60.

Compound **5** should be generally useful for the synthesis of *rac*-bis-indenyl metallocenes. However, further tuning of the steric interactions between the bis-amide directing group and the metallocene framework may be required for broader application of this strategy. For example, as described elsewhere, the reaction of $Li_2[Me_2Si(3\text{-}^tBu\text{-}C_5H_3)_2]$ with **5** yields *meso*-$Me_2Si(3\text{-}^tBu\text{-}C_5H_3)_2Zr\{PhN(CH_2)_3NPh\}$ (*meso*-**15**) in >98% yield. In this case, the extremely bulky 3-^{t}Bu substituents force the $Zr\{PhN(CH_2)_3NPh\}$ ring into an unusual envelope conformation, which results in the *meso* selectivity.[32] However, the reaction of $Li_2[Me_2Si(3\text{-}^tBu\text{-}C_5H_3)_2]$ with $Zr\{Me_3SiN(CH_2)_3NSiMe_3\}Cl_2(THF)_2$ (**16**), which contains three-dimensionally bulky N−*SiMe*$_3$ groups in place of the flat N−*Ph* groups of **5**, affords *rac*-$Me_2Si(3\text{-}^tBu\text{-}C_5H_3)_2Zr\{Me_3SiN(CH_2)_3NSiMe_3\}$ (*rac*-**17**) in high yield. The $Zr\{Me_3SiN(CH_2)_3NSiMe_3\}$ rings in **16** and *rac*-**17** have twist conformations.

The current working model for stereocontrol in these chelate-controlled metallocene syntheses is based on the hypothesis that the $Zr\{RN(CH_2)_3NR\}$ ring conformation in the stereodetermining transition state for addition of the second Cp′ ligand is similar to that in the metallocene product. While the mechanistic details of substitution of chloride by a $[Cp']^-$ group would be difficult to probe experimentally, computational studies of relevant metal amide complexes may assist in understanding and exploiting this approach to metallocene synthesis.

Experimental Section

General Procedures. All manipulations were performed under purified nitrogen in a drybox or on a high-vacuum line. Nitrogen was purified by passage through columns of activated molecular sieves and Q-5 oxygen scavenger. Toluene, benzene, tetrahydrofuran, hexamethyldisiloxane, and diethyl ether were distilled under nitrogen from sodium/benzophenone ketyl. Alternatively, toluene, benzene, pentane, and hexanes were purified by passage through columns of activated alumina and BASF R3-11 oxygen-removal catalyst. CH_2Cl_2, CD_2Cl_2, $CDCl_3$, and DMSO were distilled under nitrogen from P_2O_5 or CaH_2. THF-d_8, C_6D_6, and toluene-d_8 were distilled under nitrogen from sodium/benzophenone ketyl, degassed, and stored under vacuum. $ZrCl_4$ was purchased from Cerac and sublimed before use. *N*-Methylaniline, 1,3-dibromopropane, aniline, NaN_3, $PhBCl_2$, and $PhHN(CH_2)_2NHPh$ were purchased from Aldrich and used as received. *N*,*N*′-Diphenylpropanediamine ($PhNH(CH_2)_3NHPh$) was prepared by a literature procedure[12] or as described below. The bis-indenes $(1\text{-indenyl})_2SiMe_2$,[10d,33] $(2\text{-Me-indenyl})_2SiMe_2$,[34] $(2\text{-Me-4,5-benz-1-indenyl})_2SiMe_2$,[3b] 1,2-(1-indenyl)$_2$ethane,[10b,35] and $(2\text{-Me-4-Ph-indenyl})_2SiMe_2$[3a] were prepared by literature procedures. These compounds were converted to the corresponding $Li_2[XBI'](Et_2O)$ salts **7a**−**e** in 80−90% yield by reaction with ^{n}BuLi in Et_2O (2 equiv, 23 °C, overnight in Et_2O). Salts **7a**−**e** were isolated by filtration, washed with hexane, and dried under vacuum. Li[NMePh] was prepared by reaction of *N*-methylaniline with ^{n}BuLi in hexanes, isolated by filtration, washed with hexanes and pentane, and dried under vacuum.

NMR spectra were recorded on Bruker AMX-360, AMX-400, or AMX-500 spectrometers in flame-sealed or Teflon-valve tubes at ambient probe temperature unless otherwise indicated. ^{1}H and ^{13}C chemical shifts are reported relative to $SiMe_4$ and were determined by reference to the residual ^{1}H and ^{13}C solvent resonances. Coupling constants are given in hertz. Elemental analyses were performed by Desert Analytics Laboratory (Tucson, AZ) or Midwest Microlabs (Indianapolis, IN). ESI-MS experiments were performed with a Hewlett-Packard 1100MSD instrument using direct injection via a syringe pump (ca. 10^{-6} M solutions). Good agreement between observed and calculated isotope patterns was observed in all cases. The listed *m*/*z* value corresponds to the most intense peak in the isotope pattern.

1,3-Diazidopropane (3).[13] A flask was charged with DMSO (1 L) and NaN_3 (19.0 g, 0.290 mol). The slurry was stirred at room temperature until no solid was observed (24−72 h). The solution was sparged with nitrogen for 2 h while stirring was maintained. 1,3-Dibromopropane (26.8 g, 0.130 mol) was added by syringe, and the mixture was stirred overnight at room temperature. Water was added in portions (5 × 100 mL) while allowing the reaction mixture to cool to room temperature between portions. The mixture was extracted with (3 × 300 mL) of Et_2O. The extracts were combined and washed with water (2 × 500 mL) and brine (300 mL). The ether layer was separated and dried over $MgSO_4$. The solvent was removed under vacuum to yield a clear oil (16.4 g, 0.130 mol, 100%). ^{1}H NMR ($CDCl_3$): δ 3.43 (t, J = 6, 4H,), 1.84 (pentet, J = 6, 2H).

Malonaldehyde Bis(phenylimine).[36] A flask was charged with malonaldehyde bis(phenylimine) monohydrochloride ($(PhN{=}CHCH_2\text{-}CH{=}NPh)\cdot HCl$, 11.9 g, 46.0 mmol) and deionized water (900 mL). Aqueous NaOH (5.0 M, 100 mL) was added. The mixture was stirred for 12 h at room temperature. The solid was collected by filtration, washed with water (100 mL), and dried under vacuum overnight to yield a yellow powder (10.6 g, 100%). ^{1}H NMR (DMSO-d_6): δ 9.60 (br s, 1H, N*H*), 7.94 (br s, 2H, NHC*H*), 7.27 (br t, 4H, Ph), 7.00 (br s, 4H, Ph), 6.96 (br s, 2H, Ph), 5.78 (br t, 1H, NHCHC*H*).

***N*,*N*′-Diphenyl-1,3-propanediamine (1).**[14] **Method A: *N*,*N*′-Diphenyl-1,3-propanediamine·2HCl.** A flask was charged with toluene (50 mL) and 1,3-diazidopropane (6.30 g, 50.0 mmol). A separate flask was charged with toluene (50 mL) and $PhBCl_2$ (17.47 g, 110.0 mmol). Both flasks were cooled to 0 °C. The diazide solution was added dropwise (*with extreme caution!*) to the $PhBCl_2$ solution via cannula. Immediate gas evolution was observed. The mixture was stirred for 24 h, during which time the flask was allowed to warm to room temperature. Methanol (16.6 g, 500 mmol) was added by syringe, and the mixture was stirred for 45 min. Ether (100 mL) was added to facilitate precipitation. The precipitate was collected by filtration, washed with cold ether, and dried overnight under vacuum to yield *N*,*N*′-diphenyl-1,3-propanediamine·2HCl as a pale orange solid (12.5 g, 41.44 mmol, 83%). ^{1}H NMR (D_2O): δ 7.40 (m, 6H, Ph), 7.26 (m, 4H, Ph), 3.37 (m, 4H, CH_2), 1.95 (m, 2H, CH_2). For conversion of *N*,*N*′-diphenyl-1,3-propanediamine·2HCl to *N*,*N*′-diphenyl-1,3-propanediamine, a solution of *N*,*N*′-diphenyl-1,3-propanediamine·2HCl (8.72 g, 29.1 mmol) in deionized H_2O (200 mL) was stirred and aqueous NaOH (5.0 M, 120 mL) was added. The mixture was stirred for 2 min and extracted with Et_2O (4 × 250 mL). The Et_2O extracts were combined, washed with H_2O (2 × 250 mL), dried over $MgSO_4$, and concentrated under vacuum to yield an amber oil (6.45 g, 97%). ^{1}H NMR ($CDCl_3$): δ 7.23 (t, J = 8, 4H, Ph), 6.74 (t, J = 8, 2H, Ph), 6.67 (d, J = 8, 4H, Ph), 3.74 (s, 2H, NH), 3.32 (t, J = 4, 4H, CH_2), 1.96 (pentet, J = 4, 2H, CH_2).

***N*,*N*′-Diphenyl-1,3-propanediamine (1). Method B.**[15] A flask was charged with aniline (98.1 g, 1.05 mol) and heated to 130 °C. 1,3-Dibromopropane (52.7 g, 0.261 mol) was added over a 30 min period while the temperature was maintained between 130 and 160 °C. The mixture was stirred for 2 h at 135 °C. The flask was cooled to 80 °C, and aqueous KOH (6.2 M, 100 mL) was added while the stirring was maintained. The mixture was extracted with Et_2O (150 mL). The Et_2O extract was dried over $MgSO_4$, filtered, and concentrated under vacuum.

(32) LoCoco, M. D.; Jordan, R. F. *Organometallics* **2003**, *22*, 5498.
(33) (a) Marechal, E.; Tortal, J. P. *C. R. Acad. Sci. Paris* **1968**, 267, 467. (b) Sommer, L. H.; Marans, N. S. *J. Am. Chem. Soc.* **1951**, *73*, 5135.
(34) Spaleck, W.; Antberg, M.; Rohrmann, J.; Winter, A.; Bachmann, B.; Kiprof, P.; Behm, J.; Herrmann, W. A. *Angew. Chem., Int. Ed. Engl.* **1992**, *31*, 1347.
(35) (a) Collins, S.; Kuntz, B. A.; Taylor, N. J.; Ward, D. G. *J. Organomet. Chem.* **1988**, 342, 21. (b) Lee, I. M.; Gauthier, W. J.; Ball. J. M.; Iyengar, B.; Collins, S. *Organometallics* **1992**, *11*, 2115.
(36) (a) Barry, W. J.; Finar, I. L.; Mooney, E. F. *Spectrochim. Acta* **1965**, *21*, 1095. (b) Fisher, K. J. *Tetrahedron Lett.* **1970**, 30, 2613.

The concentrate was heated to 60 °C under vacuum overnight. The remaining oil was distilled under vacuum (7.5×10^{-4} mm); excess aniline was removed in the first fraction, and the product was obtained as a clear colorless oil at 150 °C as the second fraction (33 g, 56%).

***N,N′*-Diphenyl-1,3-propanediamine (1). Method C.**[16] A flask was charged with Na metal (21.2 g, 0.920 mol) and 2-propanol (111 g, 1.85 mol). The flask was cooled to 0 °C. A second flask was charged with malonaldehyde bis(phenylimine) (20.55 g, 92.39 mmol) and THF (400 mL), and this solution was cannula-transferred to the flask containing the Na and 2-propanol. A mild exotherm and gas evolution were observed. The mixture was stirred for 20 h at room temperature. The mixture was cannula-transferred to a flask containing 400 g of ice and stirred. After the ice melted, the mixture was extracted with ether (3×200 mL). The extracts were combined and dried over $MgSO_4$. The volatiles were removed under vacuum to yield an amber oil (19.98 g, 95%). This material was pure by ^{1}H NMR and was used in subsequent studies. The oil can be recrystallized from a solution of toluene layered with hexanes to yield clear crystals.

Li_2[PhN(CH_2)$_3$NPh] (4). A flask was charged with benzene (200 mL) and *N,N′*-diphenyl-1,3-propanediamine (**1**, 16.6 g, 73.4 mmol). The flask was cooled in an ice−water bath, and a solution of ^{n}BuLi in hexanes (91.8 mL, 1.60 M, 147 mmol) was added by syringe. The mixture was stirred for 8 h at room temperature and filtered through a glass frit to afford a white solid, which was dried under vacuum (17.4 g, 99%). ^{1}H NMR (THF-d_8): δ 6.76 (t, $J = 8$, 4H, Ph), 6.28 (d, $J = 8$, 4H, Ph), 5.94 (t, $J = 8$, 2H, Ph), 3.04 (t, $J = 6$, 4H, CH_2), 1.94 (m, 2H, CH_2).

Zr{PhN(CH_2)$_3$NPh}$_2$ (6). A slurry of $ZrCl_4$ (1.23 g, 5.29 mmol) in toluene (70 mL) was prepared, and solid Li_2[PhN(CH_2)$_3$NPh] (**4**, 2.52 g, 10.6 mmol) was added in several portions over 2 h at 23 °C. The mixture was stirred at 23 °C for 2 d. The mixture was cooled to −196 °C, and THF (35 mL) was added by vacuum transfer. The mixture was stirred at 23 °C for 1.5 h. The volatiles were removed under vacuum, and benzene (50 mL) was added by cannula. The mixture was stirred for 30 min and filtered. The volatiles were removed under vacuum. The residue was dissolved in benzene (20 mL), and the volatiles were removed under vacuum. This process was repeated twice. The resulting solid was washed with pentane (50 mL) and dried under vacuum (2.10 g, 73%). Anal. Calcd for $C_{30}H_{32}N_4Zr$: C, 66.74; H, 5.99; N, 10.38. Found: C; 66.93; H, 6.12; N, 10.08. ^{1}H NMR (THF-d_8): δ 7.04 (t, $J = 8$, 4H, *m*-Ph), 6.78 (d, $J = 8$, 4H, *o*-Ph), 6.63 (t, $J = 8$, 2H, *p*-Ph), 3.68 (t, $J = 5$, 4H, CH_2), 2.29 (pentet, $J = 5$, 2H, CH_2).

Zr{PhN(CH_2)$_3$NPh}Cl_2(THF)$_2$ (5). Method A. A flask was charged with Zr{PhN(CH_2)$_3$NPh}$_2$ (**6**, 1.10 g, 2.04 mmol) and $ZrCl_4$ (0.476 g, 2.04 mmol), and THF (30 mL) and Et_2O (30 mL) were added by vacuum transfer at −78 °C. The mixture was warmed to 0 °C in an ice bath, stirred overnight, and allowed to warm to room temperature gradually. The volatiles were removed under vacuum at 23 °C to yield a yellow solid (1.77 g, 100%).[37] Anal. Calcd for $C_{23}H_{32}Cl_2N_2O_2Zr$: C, 52.05; H, 6.09; N, 5.28. Found: C, 51.79; H, 6.21; N, 5.19. ^{1}H NMR (C_6D_6): δ 7.45 (d, $J = 8$, 4H, Ph), 7.20 (t, $J = 8$, 4H, Ph), 6.83 (t, $J = 8$, 2H, Ph), 4.03 (t, $J = 6$, 4H, CH_2N), 3.71 (br s, 8H, THF), 1.88 (m, 2H, CH_2), 1.03 (br s, 8H, THF). ^{13}C{^{1}H} NMR (benzene-d_6): δ 153.7, 128.8, 121.5, 121.4, 73.0, 54.4, 29.7, 25.1. Crystals for X-ray diffraction were obtained by layering hexane onto a solution of **5** in benzene and allowing the layers to mix by slow diffusion.

Zr{PhN(CH_2)$_3$NPh}Cl_2(THF)$_2$ (5). Method B. A flask was charged with $ZrCl_4$ (8.75 g, 36.8 mmol) and Li_2[PhN(CH_2)$_3$NPh] (**4**, 8.57 g, 36.8 mmol). A premeasured mixture of THF and Et_2O (1:1 by volume, 400 mL) was added by vacuum transfer at −196 °C from sodium/benzophenone. The mixture was placed in an ice bath at 0 °C and stirred for 27 h, during which time the mixture was allowed to warm to room temperature. The volatiles were removed under vacuum at 30 °C to yield a yellow solid. Benzene (300 mL) was added by vacuum transfer at −196 °C from sodium/benzophenone, and the mixture was stirred for 2 h at room temperature. The mixture was filtered through a medium-porosity glass frit (10−20 μm pore size), and the volatiles were removed from the filtrate under vacuum at 30 °C. Toluene (300 mL) was added by vacuum transfer at −196 °C, and the mixture was stirred overnight. The mixture was filtered through Celite. The flask was washed with additional toluene (200 mL), and the wash was passed through the Celite column. The filtrate and wash were combined and concentrated to 80 mL under vacuum at 35 °C. THF (5.0 mL) was added, and the solution was stirred for 1 h. Hexanes (380 mL) were added while the mixture was stirred to yield a yellow precipitate. The flask was cooled to −35 °C for 24 h. The yellow solid was collected by filtration and dried under vacuum (16.9 g, 86%).

***rac*-(SBI)Zr{PhN(CH_2)$_3$NPh} (*rac*-8a).** A flask was charged with Li_2[(1-indenyl)$_2$SiMe$_2$](Et_2O) (**7a**, 3.23 g, 8.62 mmol) and Zr{PhN(CH_2)$_3$NPh}Cl_2(THF)$_2$ (**5**, 4.92 g, 8.62 mmol). Et_2O (300 mL) was added by vacuum transfer at −196 °C. The mixture was allowed to warm to room temperature and stirred for 11 h. The volatiles were removed under vacuum to yield a red solid. Benzene (200 mL) was added by vacuum transfer at −196 °C, and the mixture was stirred for 2 h at room temperature. The mixture was filtered through a medium-porosity glass frit, and the filtrate was dried under vacuum at 30 °C for 3 h to yield a red solid (4.75 g, 92%). Crystals of *rac*-**8a**·C_7H_8 for X-ray diffraction were obtained by layering hexamethyldisiloxane onto a solution of *rac*-**8a** in toluene and allowing the layers to mix by slow diffusion. Anal. Calcd for $C_{35}H_{34}N_2SiZr$: C, 69.83; H, 5.69 N, 4.65. Found: C, 69.49; H, 5.81; N, 4.25. ^{1}H NMR (C_6D_6): δ 7.60 (d, $J = 8$, 2H), 7.24 (t, $J = 7$, 4H), 6.97 (d, $J = 8$, 2H), 6.89 (t, $J = 6$, 2H), 6.78 (t, $J = 6$, 2H), 6.52 (d, $J = 6$, 2H), 6.50 (d, $J = 3$, 2H), 6.45 (d, $J = 8$, 4H), 6.36 (d, $J = 3$, 2H), 3.18 (dt, $J = 9$, 3, 2H), 3.04 (pentet, $J = 7$, 2H), 1.39 (m, 2H), 0.80 (s, 6H). ^{13}C{^{1}H} NMR (C_6D_6): δ 159.6, 130.6, 128.8, 128.3, 126.0, 125.3, 124.7, 123.4, 118.8, 118.6, 115.8, 111.9, 92.4 55.37, 25.54, −1.55.

***rac*-(MSBI)Zr{PhN(CH_2)$_3$NPh} (*rac*-8b).** A flask was charged with Zr{PhN(CH_2)$_3$NPh}Cl_2(THF)$_2$ (**5**, 1.01 g, 3.07 mmol) and Li_2[MSBI](Et_2O) (**7b**, 1.63 g, 3.07 mmol), and Et_2O (75 mL) was added by vacuum transfer at −196 °C. The mixture was warmed to −78 °C and stirred for 17 h, during which time it was allowed to warm to 23 °C. The volatiles were removed under vacuum, and benzene (50 mL) was added by vacuum transfer at −196 °C. The mixture was warmed to 23 °C, stirred for 2 h, and filtered through a medium-porosity glass frit. The volatiles were removed from the filtrate under vacuum to yield a red solid (1.86 g, 96%). ^{1}H NMR (C_6D_6): δ 7.74 (d, $J = 7$, 2H), 7.23 (m, 6H), 6.96 (m, 4H), 6.72 (m, 2H), 6.55 (d, $J = 7$, 4H), 6.2 (s, 2H, indenyl H3), 3.60 (dt, $J = 14$, 7; 2H, CH_2), 3.05 (dt, $J = 11$, 4, 2H, CH_2), 2.01 (s, 6H, 2-Me), 1.24 (m, 2H, CH_2), 0.88 (s, 6H, $SiMe_2$). ^{13}C{^{1}H} NMR (C_6D_6): δ 161.8, 129.5, 129.4, 128.5, 125.5, 124.6, 124.4, 124.1, 123.4, 121.8, 116.0, 93.1, 59.7, 22.9, 19.0, 2.2.

***rac*-(MBSBI)Zr{PhN(CH_2)$_3$Ph} (*rac*-8c).** A flask was charged with Zr{PhN(CH_2)$_3$Ph}Cl_2(THF)$_2$ (**5**, 0.567 g, 1.00 mmol) and Li_2[MBSBI](Et_2O) (**7c**, 0.511 g, 1.00 mmol), and Et_2O (50 mL) was added by vacuum transfer. The mixture was stirred for 18 h at 23 °C. The volatiles were removed under vacuum, and the resulting solid was taken up in benzene (50 mL), stirred for 20 min, and filtered. The volatiles were removed from the filtrate under vacuum to afford a red solid (0.75 g, 99%). This material was recrystallized from toluene/hexane (1:10 v/v) at −20 °C (0.68 g, 90%). A 92% yield was obtained when the reaction was performed on a 3 mmol scale. Crystals for X-ray diffraction were obtained by crystallization from toluene/hexanes. Anal. Calcd for $C_{45}H_{42}N_2SiZr$: C, 73.74; H, 5.81; N, 3.83. Found: C, 73.82; H, 5.92; N, 3.34. ^{1}H NMR (C_6D_6): δ 7.89 (d, $J = 8$, 2H), 7.82 (d, $J = 8$, 2H), 7.52 (m, 2H), 7.33 (d, $J = 8$, 2H, indenyl), 7.20 (t, $J = 8$, 4H), 7.13 (m, obscured by solvent), 6.95 (t, $J = 7$, 2H), 6.72 (s, 2H), 6.59 (d, $J = 9$, 4H), 3.45 (dt, $J = 14$, 7, 2H, CH_2), 2.18 (s, 6H, Me), 2.12 (dt, $J = 14$, 4, 2H, CH_2), 0.99 (s, 6H, $SiMe_2$), 0.89 (br s, 2H, CH_2). ^{13}C{^{1}H}

(37) Oxidation/hydrolysis of **5** in C_6D_6 yields an insoluble solid and releases THF. Therefore, it is imperative that dry, anaerobic conditions be used to determine the THF content of **5**.

NMR (C_6D_6): δ 162.1, 131.4, 130.2, 128.9, 128.6, 128.3, 126.6, 126.4, 126.2, 126.1, 125.8, 124.7, 124.4, 123.4, 121.9, 116.7, 98.8, 56.8, 21.5, 18.9, 2.2.

***rac*-(MPSBI)Zr{PhN(CH$_2$)$_3$NPh} (*rac*-8d).** A flask was charged with Li_2[(2-methyl-4-phenyl-indenyl)$_2$SiMe$_2$](Et_2O) (**7d**, Li_2[MPSBI]-(Et_2O), 3.15 g, 5.68 mmol) and Zr{PhN(CH$_2$)$_3$NPh}Cl$_2$(THF)$_2$ (**5**, 3.16 g, 5.68 mmol), and Et_2O (225 mL) was added by vacuum transfer at −196 °C. The mixture was allowed to warm to room temperature and stirred for 19 h. The volatiles were removed under vacuum to yield a red solid. Benzene (150 mL) was added by cannula transfer, and the mixture was stirred for 15 min at room temperature. The mixture was filtered through a medium-porosity glass frit, and the filtrate was dried under vacuum at 30 °C for 2 h to yield a red solid (4.43 g, 99%). A fraction of this material (100 mg) was recrystallized from benzene/hexanes (yield 71 mg). Anal. Calcd for $C_{49}H_{46}N_2SiZr$: C, 75.19; H, 5.94; N, 3.58. Found: C, 74.41; H, 6.23; N, 3.11. ^{1}H NMR (C_6D_6): δ 7.80 (d, J = 7, 2H), 7.45 (d, J = 7, 4H), 7.18−7.13 (m, obscured by solvent), 7.00 (m, 4H), 6.98 (t, J = 7, 4H), 6.71 (s, 2H), 6.40 (d, J = 7, 4H), 3.34 (dt, J = 14, 9, 2H, CH_2), 2.75 (dt, J = 14, 3, 2H, CH_2), 2.11 (s, 6H, 2-Me), 0.98 (s, 6H, $SiMe_2$), 0.88 (m, 2H, CH_2). ^{13}C{^{1}H} NMR (C_6D_6): δ 162.1, 141.1, 137.8 131.9, 129.3, 129.1, 128.5, 128.3, 128.0 (obscured by solvent), 127.4, 125.0, 124.6, 123.9, 123.8, 122.2, 116.3, 92.9, 59.7, 21.7, 19.1, 2.4.

***rac*-(EBI)Zr{PhN(CH$_2$)$_3$NPh} (*rac*-8e).** A flask was charged with Li_2[EBI](Et_2O) (**7e**, 0.94 g, 2.73 mmol) and Zr{PhN(CH$_2$)$_3$NPh}Cl$_2$-(THF)$_2$ (**5**, 1.45 g, 2.73 mmol), and Et_2O (150 mL) was added by vacuum transfer at −196 °C. The mixture was allowed to warm to room temperature and stirred for 11 h. The volatiles were removed under vacuum to yield a red solid. Benzene (100 mL) was added by vacuum transfer at −196 °C, and the mixture was warmed to room temperature and stirred for 2 h. The mixture was filtered through a medium-porosity glass frit and concentrated to 50 mL under vacuum. Pentane (150 mL) was added, and the mixture was filtered through a medium-porosity glass frit. The filtrate was dried under vacuum at 30 °C for 12 h to yield a red solid (1.21 g, 78%). Anal. Calcd for $C_{35}H_{32}N_2$-Zr: C, 73.51; H, 5.64; N, 4.90. Found: C, 73.52; H, 5.83; N, 4.91. ^{1}H NMR (C_6D_6): δ 7.44 (d, J = 9, 2H), 7.26 (t, J = 8, 4H), 6.90 (m, 4H), 6.85 (t, J = 8, 2H), 6.53 (t, J = 8, 2H), 6.38 (d, J = 8, 4H), 6.26 (d, J = 3, 2H), 5.96 (d, J = 3, 2H), 3.20 (m, 4H), 3.06 (pent, J = 9, 4H), 1.34 (m, 2H). ^{13}C{^{1}H} NMR: δ 159.6, 128.5, 128.3, 125.3, 124.9, 124.1, 120.5, 119.2, 118.7, 117.6, 112.2, 104.5, 54.7, 28.3, 25.3.

***rac*-(SBI)ZrCl$_2$ (*rac*-9a).** A flask was charged with *rac*-(SBI)Zr-{PhN(CH$_2$)$_3$NPh} (**8a**, 0.667 g, 1.10 mmol), and benzene (45 mL) was added by cannula at room temperature. The mixture was stirred, and a solution of HCl in Et_2O (1.0 M, 2.20 mL, 2.20 mmol) was added by syringe. The mixture was stirred at room temperature for 1 h, and the volatiles were removed under vacuum to yield a viscous yellow oil. The oil was taken up in benzene (20 mL) to yield a yellow suspension, which was filtered through a fine-porosity glass frit to yield a yellow solid. This material was washed with 20 mL of hexanes and dried under vacuum to yield pure **9a** (0.402 g, 89%).[20] ^{1}H NMR (CD_2Cl_2): δ 7.59 (d, J = 8, 2H), 7.55 (d, J = 8, 2H), 7.38 (m, 2H), 7.13 (m, 2H), 6.91 (d, J = 3, 2H, indenyl H2 or H3), 6.14 (d, J = 3, 2H, indenyl H2 or H3), 1.15 (s, 6H, $SiMe_2$). ^{13}C{^{1}H} NMR (CD_2Cl_2): δ 133.9, 127.8, 127.1, 126.6, 124.9, 118.3, 118.1, 90.2, −1.6. No *meso*-**9a** was detected.

***rac*-(MSBI)ZrCl$_2$ (*rac*-9b). Method A.** A flask was charged with Zr{PhN(CH$_2$)$_3$NPh}Cl$_2$(THF)$_2$ (**5**, 0.585 g, 1.10 mmol) and Li_2[MSBI]-(Et_2O) (**7b**, 0.444 g, 1.10 mmol), and Et_2O (50 mL) was added by vacuum transfer. The mixture was stirred for 22 h at 23 °C. The volatiles were removed under vacuum. The resulting solid was taken up in benzene (40 mL) and filtered. The volatiles were removed from the filtrate under vacuum to afford a red solid. The solid was taken up in benzene (30 mL) and filtered. The volatiles were removed from the filtrate under vacuum to afford a red solid (0.638 g). A portion of the solid (0.334 g) was dissolved in CH_2Cl_2/Et_2O (30 mL, 1:1 by volume). The solution was cooled to −78 °C, and HCl (1.0 mL of a 1.0 M solution in Et_2O, 1.0 mmol) was added. The mixture was stirred for 10 min at −78 °C. The red solution turned into a yellow-orange slurry. The volatiles were removed under vacuum. The yellow-orange solid was washed with hexanes (20 mL) and benzene (2 × 10 mL) and dried under vacuum (yield 0.18 g, 73%).

***rac*-(MSBI)ZrCl$_2$ (*rac*-9b). Method B.** A flask was charged with $ZrCl_4$ (1.27 g, 5.45 mmol) and Li_2[PhN(CH$_2$)$_3$NPh] (**4**, 1.30 g, 5.46 mmol), and THF (40 mL) and Et_2O (40 mL) were added by vacuum transfer at −78 °C. The mixture was stirred for 32 h at 23 °C. The volatiles were removed under vacuum, affording a yellow oily solid. Benzene (10 mL) was added, and the mixture was stirred for 10 min. The volatiles were removed under vacuum, yielding a yellow solid. Li_2[MSBI](Et_2O) (**7b**, 2.20 g, 5.45 mmol) was added, and Et_2O (60 mL) was added by vacuum transfer at −78 °C. The mixture was stirred for 17 h at 23 °C to afford a red slurry. The volatiles were removed under vacuum. Toluene (50 mL) was added, and the resulting slurry was stirred for 2 h and filtered to remove LiCl. The red filtrate was cooled to −78 °C, and HCl (12 mL of 1.0 M solution in Et_2O, 12 mmol) was added. The mixture was stirred for 1 h at −78 °C, warmed to 23 °C, and stirred for 20 min. The mixture was cooled to −78 °C and filtered to yield a yellow solid, which was dried under vacuum and shown to be pure *rac*-(MSBI)$ZrCl_2$ by ^{1}H NMR (2.05 g, 76% based on $ZrCl_4$). Anal. Calcd for $C_{22}H_{22}Cl_2SiZr$: C, 55.43; H, 4.66. Found: C, 54.93; H, 4.65. ^{1}H NMR (CD_2Cl_2): δ 7.68 (d, J = 8, 2H, indenyl), 7.48 (d, J = 8, 2H, indenyl), 7.35 (m, 2H, indenyl), 7.01 (m, 2H, indenyl), 6.78 (s, 2H, indenyl H3), 2.21 (s, 6H, 2-Me), 1.30 (s, 6H, $SiMe_2$).

***rac*-(MBSBI)ZrCl$_2$ (*rac*-9c).** A flask was charged with *rac*-(MBSBI)Zr{PhN(CH$_2$)$_3$NPh} (**8c**, 0.640 g, 0.875 mmol), and Et_2O (100 mL) was added by vacuum transfer at −78 °C. The mixture was stirred, and a solution of HCl in Et_2O (1.0 M, 1.83 mL, 1.83 mmol) was added by syringe. The mixture was stirred at −78 °C for 20 min, allowed to warm to room temperature, and stirred for 6 h. The volatiles were removed under vacuum to yield a yellow solid. Benzene (30 mL) was added by vacuum transfer at −196 °C, and the mixture was warmed to room temperature and stirred for 30 min. The mixture was filtered through a medium-porosity glass frit, and the volatiles were removed from the filtrate under vacuum at 30 °C. The resulting yellow solid was dried under vacuum (0.41 g, 83%). A ^{1}H NMR spectrum established that this material was pure *rac*-(MBSBI)$ZrCl_2$.[3b] ^{1}H NMR (CD_2Cl_2): δ 7.95 (d, J = 8, 2H), 7.79 (d, J = 8, 2H), 7.63 (d, J = 9, 2H), 7.57 (t, J = 6, 2H), 7.52 (t, J = 6, 2H), 7.37 (d, J = 9, 2H), 7.26 (s, 2H), 2.36 (s, 6H, Me), 1.36 (s, 6H, Me).

***rac*-(MPSBI)ZrCl$_2$ (*rac*-9d).** A flask was charged with *rac*-(MPSBI)Zr{PhN(CH$_2$)$_3$NPh} (**8d**, 1.66 g, 2.12 mmol), and Et_2O (100 mL) was added by vacuum transfer at −78 °C. A solution of HCl in Et_2O (1.0 M, 4.24 mL, 4.2 mmol) was added by syringe while the mixture was stirred. The mixture was stirred at −78 °C for 20 min and then allowed to warm to room temperature overnight while the stirring was maintained. The mixture was filtered through a medium-porosity glass frit. The volatiles were removed under vacuum to yield a yellow solid which was dried under vacuum and shown to be pure *rac*-(MPSBI)$ZrCl_2$ by ^{1}H NMR (0.826 g, 83%).[3a] ^{1}H NMR (CD_2Cl_2): δ 7.70 (d, J = 9, 2H), 7.62 (m, 4H), 7.45 (m, 4H), 7.35 (m, 4H), 7.13 (dd, J = 8, 2, 2H), 6.92 (s, 2H), 2.25 (s, 6H, 2-Me), 1.36 (s, 6H, $SiMe_2$).

***rac*-(EBI)ZrCl$_2$ (*rac*-9e).** A flask was charged with *rac*-(EBI)Zr-{PhN(CH$_2$)$_3$NPh} (*rac*-**8e**, 1.15 g, 2.01 mmol), and benzene (50 mL) was added by cannula at room temperature. The mixture was stirred, and a solution of HCl in Et_2O (1.0 M, 3.95 mL, 1.95 mmol) was added by syringe. The mixture was stirred at room temperature for 20 min, concentrated under vacuum to 25 mL, and filtered through a medium-porosity glass frit to yield a yellow solid. The solid was dried under vacuum, yielding pure *rac*-**9e** (0.680 g, 81%). ^{1}H NMR (CD_2Cl_2): δ 7.69 (d, J = 8, 2H), 7.43 (d, J = 8, 2H), 7.30 (t, J = 7, 2H), 7.18 (t, J = 7, 2H), 6.55 (d, J = 3, 2H), 6.23 (d, J = 3, 2H), 3.74 (m, 4H, CH_2CH_2). No *meso*-**9e** was detected by NMR.

$Cp_2Zr\{PhN(CH_2)_3NPh\}$ (10). A flask was charged with Cp_2ZrCl_2 (1.26 g, 4.31 mmol) and $Li_2[PhN(CH_2)_3NPh]$ (**5**, 1.03 g, 4.32 mmol), and Et_2O (100 mL) was added by vacuum transfer at −196 °C. The mixture was warmed to −78 °C and then stirred overnight while being allowed to warm to room temperature. The volatiles were removed under vacuum, and toluene (100 mL) was added by vacuum transfer at −196 °C. The mixture was warmed to room temperature, stirred for 1 h, and filtered through a medium-porosity glass frit. The volatiles were removed under vacuum to yield a red solid (1.72 g, 90%). This material was recrystallized from benzene/hexamethyldisiloxane to afford X-ray-quality crystals. Anal. Calcd for $C_{25}H_{26}N_2Zr$: C, 67.37; H, 5.88; N, 6.29. Found: C, 67.33; H, 5.94; N, 6.21. ^{1}H NMR (C_6D_6): δ 7.24 (t, J = 8, 4H), 6.92 (t, J = 8, 2H), 6.55 (d, J = 8, 4H), 5.82 (s, 10H), 3.33 (t, J = 6, 2H), 1.44 (p, J = 6, 2H). $^{13}C\{^1H\}$ NMR (C_6D_6): δ 162.0, 128.4, 120.6, 119.4, 110.7, 54.5, 26.9.

$Zr(NMePh)_4$. A slurry of Li[NMePh] (4.26 g, 37.7 mmol) in toluene (150 mL) was prepared, and solid $ZrCl_4$ (2.20 g, 9.44 mmol) was added in several portions over 2 h at room temperature. The mixture was stirred at 23 °C for 25 h. The volatiles were removed under vacuum, and the residue was extracted with hexanes (50 mL) and benzene (2 × 70 mL). The extracts were combined, and the volatiles were removed under vacuum, yielding pure $Zr(NMePh)_4$ as a pale yellow powder (2.18 g, 45%). Anal. Calcd for $C_{28}H_{32}N_4Zr$: C, 65.19; H, 6.27; N, 10.86. Found: C, 64.82; H, 6.40; N, 10.47. ^{1}H NMR (C_6D_6): δ 7.11 (t, J = 7.0, 2H, Ph), 6.86 (d, J = 7.0, 2H, Ph), 6.77 (t, J = 7.0, 1H, Ph), 2.97 (s, 3H, NMe). $^{13}C\{^1H\}$ NMR (C_6D_6): δ 151.9, 129.9, 120.6, 116.3, 32.8.

$Zr(NMePh)_2Cl_2(THF)_2$ (11). A flask was charged with $Zr(NMePh)_4$ (1.16 g, 2.24 mmol) and $ZrCl_4$ (0.523 g, 2.24 mmol), and Et_2O (60 mL) and THF (25 mL) were added sequentially by vacuum transfer at −78 °C. The mixture was stirred at 23 °C for 5 h and filtered to afford a yellow solid and clear yellow filtrate. The solid was dried under vacuum overnight and identified as $Zr(NMePh)_2Cl_2(THF)_2$ (1.46 g). The yellow filtrate was cooled to −60 °C for 3 d, yielding additional product as yellow crystals (0.40 g). The total yield was 80%. Crystals for X-ray diffraction were obtained by crystallization from toluene at −20 °C. Anal. Calcd for $C_{22}H_{32}Cl_2N_2O_2Zr$: C, 50.94; H, 6.23; N, 5.40. Found: C, 50.48; H, 6.51; N, 5.16. ^{1}H NMR (THF-d_8): δ 7.24 (d, J = 7.2, 2H, Ph), 7.13 (t, J = 7.2, 2H, Ph), 6.70 (t, J = 7.2, 1H, Ph), 3.61 (m, 4H, THF), 3.32 (s, 3H, NMe), 1.76 (m, 4H, THF). $^{13}C\{^1H\}$ NMR (THF-d_8): δ 154.4, 128.8, 120.0, 118.6, 67.4 (THF), 36.2 (NMe), 26.1 (THF).

***rac*- and *meso*-(MBSBI)Zr(NMePh)$_2$ (*rac*- and *meso*-12). (a) NMR Scale.** A solution of $Zr(NMePh)_2Cl_2(THF)_2$ (**11**, 0.030 g, 0.058 mmol) in C_6D_6 (0.6 mL) was added to solid Li_2[MBSBI]Et_2O (**7c**, 0.030 g, 0.059 mmol). The yellow-orange slurry was stirred for 19 h and then centrifuged upside-down to trap the LiCl at the top of the tube, and a ^{1}H NMR spectrum was recorded. The spectrum established that the product mixture consisted of *rac*-(MBSBI)$Zr(NMePh)_2$, *meso*-(MBSBI)-$Zr(NMePh)_2$, and (MBSBI)$\{Zr(NMePh)_2Cl\}_2$ in a 2:2:1.5 molar ratio. This reaction was repeated in Et_2O (17 h, 23 °C), and the product distribution was determined by removal of the solvent under vacuum and NMR analysis of the crude product in C_6D_6. The same products were observed in a 2:2:1.5 molar ratio. **(b) Preparative Scale.** A slurry of $Zr(NMePh)_2Cl_2(THF)_2$ (**11**, 0.573 g, 1.11 mmol) and Li_2[MBSBI]-(Et_2O) (**7c**, 0.531 g, 1.04 mmol) in Et_2O (80 mL) was stirred for 18 h at 23 °C. The color changed from yellow to red. The mixture was filtered to yield a red precipitate (precipitate 1) and a red filtrate. The filtrate was taken to dryness under vacuum, yielding a red solid (230 mg). NMR analysis established that the red solid contained (MBSBI)-$Zr(NMePh)_2$ (*rac*/*meso* = 7.2:1) and (MBSBI)$\{Zr(NMePh)_2Cl\}_2$ in a molar ratio of 2.3:1. This solid was recrystallized from Et_2O to afford pure (MBSBI)$Zr(NMePh)_2$ (170 mg, *rac*/*meso* = 9.5:1). Precipitate 1 from the first filtration was extracted with toluene(2 × 40 mL). The volatiles were removed from the extracts under vacuum to yield analytically pure (MBSBI)$Zr(NMePh)_2$ (*rac*/*meso* = 1:17; red solid, 208 mg). *meso*-(MBSBI)$Zr(NMePh)_2$·(1.5 benzene) (*meso*-**12**·(1.5 benzene), 100 mg) was isolated as X-ray-quality crystals by recrystallization of this material from benzene/hexanes. The mother liquor was dried under vacuum, and the residue was recrystallized from Et_2O at −45 °C to afford X-ray-quality crystals of *rac*-**12**. The total yield for (MBSBI)$Zr(NMePh)_2$ was 51%. Anal. Calcd for $C_{44}H_{42}N_2SiZr$: C, 73.58; H, 5.91; N, 3.90. Found: C, 73.48; H, 6.15; N, 3.10.

Data for *rac*-(MBSBI)Zr(NMePh)$_2$ (*rac*-12). ^{1}H NMR (C_6D_6): δ 8.10 (m, 2H), 7.79 (d, J = 8, 2H), 7.55 (m, 2H), 7.35 (d, J = 10, 2H), 7.27−7.22 (m, 8H, indenyl and Ph), 6.96 (t, J = 7.2, 2H, Ph), 6.86 (d, J = 8, 4H, Ph), 6.74 (s, 2H, indenyl H3), 2.26 (s, 6H), 2.05 (s, 6H), 0.87 (s, 6H, $SiMe_2$).

Data for *meso*-(MBSBI)Zr(NMePh)$_2$ (*meso*-12). ^{1}H NMR (C_6D_6, 50 °C): δ 7.96 (d, J = 9, 2H), 7.71 (br d, J = 8, 2H, indenyl), 7.35 (d, J = 8, 2H), 7.2−7.06 (m, partially obscured by solvent), 6.98 (t, J = 8, 2H, Ph), 6.93−6.83 (m, 3H), 6.58 (t, J = 7, 1H, Ph), 6.28 (d, J = 8, 3H), 3.87 (s, 3H, NMe), 2.21 (s, 6H, 2-Me), 1.15 (s, 3H, $SiMe_2$), 0.80 (s, 3H, $SiMe_2$), 0.17 (s, 3H, NMe).

$Li_2[PhN(CH_2)_2NPh](Et_2O)$. A solution of ^{n}BuLi in hexanes (16.3 mL, 2.5 M, 40.7 mmol) was added to a solution of $PhNHCH_2CH_2$-NHPh (4.32 g, 20.4 mmol) in Et_2O (70 mL) over 5 min at 23 °C. The resulting slurry was stirred for 48 h and filtered. The pale yellow solid was washed with hexanes (70 mL) and dried under vacuum (4.14 g, 91%). ^{1}H NMR (THF-d_8): δ 6.68 (t, J = 8, 4H, Ph), 6.36 (br s, 4H, Ph), 5.79 (t, J = 8, 2H, Ph), 3.38 (q, J = 7, 4H, Et_2O), 3.32 (br s, 4H, NCH_2), 1.12 (t, J = 7, 6H, Et_2O).

$\{Zr\{PhN(CH_2)_2NPh\}Cl_2(THF)\}_2$ (13). A slurry of $Li_2[PhN(CH_2)_2$-$NPh](Et_2O)$ (3.35 g, 10.7 mmol) in toluene (100 mL) was prepared, and solid $ZrCl_4$ (1.24 g, 5.33 mmol) was added in several portions over 1 h. The mixture was stirred at 23 °C for 42 h and then taken to dryness under vacuum, and THF (50 mL) was added to the residue. The mixture was stirred for 5 h, and the volatiles were removed under vacuum. The resulting solid was extracted with benzene (40 mL). The volatiles were removed from the extract under vacuum. The resulting solid was washed with benzene and dried under vacuum, yielding $Zr\{PhN(CH_2)_2NPh\}_2$ as a yellow solid (1.76 g, 64%). ^{1}H NMR (THF-d_8): δ 6.99 (t, J = 7.0, 8H, *m*-Ph), 6.76 (d, J = 7.0, 8H, *o*-Ph), 6.52 (t, J = 7.0, 4H, *p*-Ph), 3.91 (s, 8H, CH_2CH_2). $^{13}C\{^1H\}$ NMR (THF-d_8): δ 156.8, 128.9, 118.0 (2C), 54.3 (CH_2CH_2). A slurry of $Zr\{PhN$-$(CH_2)_2NPh\}_2$ (0.512 g, 1.00 mmol) and $ZrCl_4$ (0.233 g, 1.00 mmol) in a mixture of Et_2O (25 mL) and THF (10 mL) was stirred at 23 °C for 5.5 h. The volatiles were removed under vacuum. The resulting yellow solid was dissolved in benzene (10 mL), and the volatiles were removed under vacuum. The solid was taken up in a mixture of toluene (5 mL) and benzene (5 mL), stirred for 10 min, and filtered. The resulting yellow-orange solid was dried under vacuum (0.47 g, 63%). Crystals of **13**·CH_2Cl_2 for X-ray diffraction were obtained by diffusion of hexanes into a CH_2Cl_2 solution at 23 °C. Anal. Calcd for $C_{18}H_{22}Cl_2N_2$-OZr: C, 48.63; H, 5.00; N, 6.30; Cl, 15.95. Found: C, 48.77; H, 5.05; N, 6.15; Cl, 15.64. ^{1}H NMR (THF-d_8): δ 7.18 (t, J = 7.0, 4H, Ph), 7.05 (d, J = 7.0, 4H, Ph), 6.77 (t, J = 7.0, 2H, Ph), 4.08 (s, 4H, CH_2CH_2), 3.63 (m, 4H, THF), 1.78 (m, 4H, THF).

(MBSBI)Zr$\{PhN(CH_2)_2NPh\}$ (14). A flask was charged with $\{Zr\{PhN(CH_2)_2NPh\}Cl_2(THF)\}_2$ (**13**, 0.458 g, 1.06 mmol) and Li_2[MBSBI](Et_2O) (**7c**, 0.544 g, 1.06 mmol), and THF (50 mL) was added by vacuum transfer at −78 °C. The mixture was stirred for 9 h, during which time the bath was allowed to warm to 5 °C. The volatiles were removed under vacuum. The resulting solid was taken up in benzene (50 mL) and filtered. The precipitate was washed with benzene (10 mL). The filtrate and wash were combined, and the volatiles were removed under vacuum. The benzene extraction process was repeated, and the final solid was dried at 50 °C under vacuum to afford a red

Table 1. Summary of X-ray Diffraction Data for Zr{PhN(CH_2)$_3$NPh} Compounds **5**, *rac*-**8a**, *rac*-**8c**, and **10**

	Zr{PhN(CH_2)$_3$NPh}Cl_2(THF)$_2$ (**5**)	*rac*-(SBI)Zr{PhN(CH_2)$_3$NPh}·C_7H_8 (*rac*-**8a**·C_7H_8)	*rac*-(MBSBI)Zr{PhN(CH_2)$_3$NPh} (*rac*-**8c**)	Cp_2Zr{PhN(CH_2)$_3$NPh} (**10**)
formula	$C_{23}H_{32}Cl_2N_2O_2Zr$	$C_{42}H_{42}N_2SiZr$	$C_{45}H_{42}N_2SiZr$	$C_{25}H_{28}N_2Zr$
formula weight	530.63	694.09	730.12	445.70
crystal system	tetragonal	monoclinic	triclinic	orthorhombic
space group	$P4_2/n$	$P2_1/n$	$P\bar{1}$	$Pca2_1$
a (Å)	24.977(1)	11.972(2)	10.3355(8)	17.627(3)
b (Å)		19.648(4)	12.1037(7)	11.044(2)
c (Å)	7.8479(4)	19.648(4)	14.8777(8)	14.749(2)
α (°)			93.503(1)	
β (°)		109.265(3)	97.219(1)	
γ (°)			107.125(1)	
V (Å^3)	4895.8(4)	3351(1)	1755.1(2)	2023.9(5)
Z	8	4	2	4
T (K)	173(2)	100(2)	173(2)	100(2)
crystal color, habit	yellow, fragment	red, fragment	orange, fragment	red, fragment
GOF on F^2	0.997	1.101	1.010	1.146
R indices [$I > 2\sigma(I)$][a]	$R1 = 0.0248$, w$R2 = 0.0708$	$R1 = 0.0408$, w$R2 = 0.0923$	$R1 = 0.0453$, w$R2 = 0.0751$	$R1 = 0.0265$, w$R2 = 0.0640$
R indices (all data)[a]	$R1 = 0.0365$, w$R2 = 0.0755$	$R1 = 0.0464$, w$R2 = 0.0954$	$R1 = 0.0808$, w$R2 = 0.0814$	$R1 = 0.0267$, w$R2 = 0.0642$

[a] $R1 = \sum||F_o| - |F_c||/\sum|F_o|$; w$R2 = [\sum[w(F_o^2 - F_c^2)^2]/\sum[w(F_o^2)^2]]^{1/2}$, where $w = q[\sigma^2(F_o^2) + (aP)^2 + bP]^{-1}$.

Table 2. Summary of X-ray Diffraction Data for Zr(NMePh)$_2$ Compounds **11**, *rac*-**12**, and *meso*-**12**

	Zr(NMePh)$_2Cl_2$(THF)$_2$ (**11**)	*rac*-(MBSBI)Zr(NMePh)$_2$ (*rac*-**12**)	*meso*-(MBSBI)Zr(NMePh)$_2$·(1.5 benzene) (*meso*-**12**·(1.5 benzene))
formula	$C_{22}H_{32}Cl_2N_2O_2Zr$	$C_{44}H_{42}N_2SiZr$	$C_{53}H_{51}N_2SiZr$
formula weight	518.62	718.11	835.27
crystal system	orthorhombic	monoclinic	monoclinic
space group	*Fdd*2	$P2_1/n$	$P2_1/n$
a (Å)	31.469(6)	21.165(8)	43.912(7)
b (Å)	10.855(2)	15.453(4)	16.786(3)
c (Å)	14.079(4)	11.026(3)	11.467(2)
α (°)			
β (°)		99.97(3)	96.99(2)
γ (°)			
V (Å^3)	4809(2)	3552(2)	8390(2)
Z	8	4	8
T (K)	213(2)	213(2)	213(2)
crystal color, habit	yellow, prism	orange, prism	transparent, fragment
GOF on F^2	1.065	1.100	1.163
R indices [$I > 2\sigma(I)$][a]	$R1 = 0.0230$, w$R2 = 0.0580$	$R1 = 0.0545$, w$R2 = 0.1334$	$R1 = 0.0397$, w$R2 = 0.1056$
R indices (all data)[a]	$R1 = 0.0283$, w$R2 = 0.0597$	$R1 = 0.0865$, w$R2 = 0.1636$	$R1 = 0.0793$, w$R2 = 0.1264$

[a] $R1 = \sum||F_o| - |F_c||/\sum|F_o|$; w$R2 = [\sum[w(F_o^2 - F_c^2)^2]/\sum[w(F_o^2)^2]]^{1/2}$, where $w = q[\sigma^2(F_o^2) + (aP)^2 + bP]^{-1}$.

Table 3. Summary of X-ray Diffraction Data for Zr{PhN(CH_2)$_2$NPh} Compounds **13**, *rac*-**14**, and *meso*-**14**

	{Zr{PhN(CH_2)$_2$NPh}Cl_2(THF)}$_2$·CH_2Cl_2 (**13**·CH_2Cl_2)	*rac*-(MBSBI)Zr(PhN(CH_2)$_2$NPh) (*rac*-**14**)	*meso*-(MBSBI)Zr(PhN(CH_2)$_2$NPh) (*meso*-**14**)
formula	$C_{74}H_{92}Cl_{12}N_8O_4Zr_4$	$C_{44}H_{40}N_2SiZr$	$C_{44}H_{40}N_2SiZr$
formula weight	1947.84	716.09	716.09
crystal system	monoclinic	orthorhombic	triclinic
space group	$P2_1/c$	$P2_12_12_1$	$P\bar{1}$
a (Å)	15.6127(8)	12.8839(9)	11.7007(6)
b (Å)	23.021(1)	14.7635(5)	12.3073(7)
c (Å)	24.104(1)	17.573(1)	13.5053(7)
α (°)			72.136(1)
β (°)	105.807(1)		75.959(1)
γ (°)			67.825(1)
V (Å^3)	8335.7(7)	3342.5(4)	1696.3(2)
Z	4	4	2
T (K)	173(2)	173(2)	173(2)
crystal color, habit	yellow, fragment	red, fragment	red, fragment
GOF on F^2	1.007	0.916	1.011
R indices [$I > 2\sigma(I)$][a]	$R1 = 0.0349$, w$R2 = 0.0796$	$R1 = 0.0410$, w$R2 = 0.0527$	$R1 = 0.0319$, w$R2 = 0.0678$
R indices (all data)[a]	$R1 = 0.0655$, w$R2 = 0.0901$	$R1 = 0.0687$, w$R2 = 0.0567$	$R1 = 0.0476$, w$R2 = 0.0712$

[a] $R1 = \sum||F_o| - |F_c||/\sum|F_o|$; w$R2 = [\sum[w(F_o^2 - F_c^2)^2]/\sum[w(F_o^2)^2]]^{1/2}$, where $w = q[\sigma^2(F_o^2) + (aP)^2 + bP]^{-1}$.

solid (682 mg, 90%, *rac*/*meso* = 2:1). This material was recrystallized from toluene/hexanes and dried under vacuum to afford pure *rac*-(MBSBI)Zr{PhN(CH_2)$_2$NPh} (332 mg, 44%) as X-ray-quality crystals. Crystals of *meso*-(MBSBI)Zr(PhN(CH_2)$_2$NPh)$_2$ for X-ray analysis were grown by slow evaporation of the filtrate. Anal. Calcd for $C_{44}H_{42}N_2$-SiZr: C, 73.74; H, 5.64; N, 3.91. Found: C, 72.92; H, 5.84; N, 3.76.

Data for *rac*-(MBSBI)Zr{PhN(CH_2)$_2$NPh}. ^{1}H NMR (C_6D_6): *δ* 7.91 (d, $J = 7.0$, 2H, indenyl), 7.61 (d, $J = 8.0$, 2H, indenyl), 7.34 (d,

J = 8.0, 2H), 7.26 (t, J = 6.0, 2H), 7.11−7.06 (m, partially obscured by solvent), 7.00 (s, 2H, indenyl), 6.82 (t, J = 6.0, 2H), 6.17 (d, J = 8.0, 4H), 3.76 (d, J = 9.0, 2H, CH_2), 2.72 (d, J = 9.0, 2H, CH_2), 2.35 (s, 6H, 2-Me), 0.93 (s, 6H, $SiMe_2$).[38]

Data for *meso*-(MBSBI)Zr{PhN(CH$_2$)$_2$NPh}. ^{1}H NMR (C_6D_6, key resonances only): δ 2.18 (s, 6H, 2-Me), 1.15 (s, 3H, $SiMe_2$), 0.78 (s, 3H, $SiMe_2$).

X-ray Structure Determinations. Crystallographic data are summarized in Tables 1−3, and full details are provided in the Supporting Information. Data were collected on Bruker CCD-1000 (**5**, *rac*-**8c**, **13**, *rac*-**14**, *meso*-**14**), Bruker Smart Apex (*rac*-**8a**, **10**), or Enraf-Nonis CAD4 (**11**, *rac*-**12**, *meso*-**12**) diffractometers using Mo Kα radiation (0.71073 Å). ORTEP plots are drawn at the 50% probability level. Non-hydrogen atoms were refined with anisotropic displacement coefficients. All hydrogen atoms were included in the structure factor calculation at idealized positions and were allowed to ride on the neighboring atoms with relative isotropic displacement coefficients, with the exception of compound **11**, for which the coordinates and isotropic displacement coefficients for H7A, H7B, and H7C were refined. The asymmetric unit of *meso*-**12**·(1.5 benzene) contains two unique molecules whose structures are very similar. The asymmetric unit of **13**·CH_2Cl_2 contains two molecules of **13**, which differ in the placement of the terminal chloride ligands (mutually syn or anti relative to the Zr- -Zr vector) but are otherwise structurally very similar. *rac*-**14** crystallizes as a merohedral twin in a 69:31 ratio.

(38) A similar reaction of **13** and Li_2[MPSBI](Et_2O) in Et_2O gave a 1:3 mixture of *rac*- and *meso*-(MPSBI)Zr{PhN(CH_2)$_2$NPh}.

Acknowledgment. This work was supported by the National Science Foundation (CHE-0212210). The Albemarle Corp. provided additional support. We thank Drs. Dale Swenson (University of Iowa), Ian Steele (University of Chicago), and Ilia Guzei (University of Wisconsin) for X-ray structure determinations.

Supporting Information Available: X-ray crystallographic data for **5**, *rac*-**8a**, *rac*-**8c**, **10**, **11**, *rac*-**12**, *meso*-**12**, **13**, *rac*-**14**, and *meso*-**14** (CIF). This material is available free of charge via the Internet at http://pubs.acs.org.

JA046629+